Finite Amplitude Thermal Convection with Spatially Modulated Boundary Temperatures

by

D. N. Riahi
Department of Theoretical and Applied Mechanics
University of Illinois at Urbana-Champaign
Urbana, Illinois 61801

Abstract

Finite amplitude thermal convection in a fluid layer between two horizontal walls with different fixed mean temperatures is considered when spatially modulated temperatures with amplitudes L_l^* and L_u^* are prescribed at the lower and upper walls, respectively. The nonlinear steady problem is solved by a perturbation technique, and the preferred mode of convection is determined by a stability analysis. For resonant wavelength excitation case, regular or non-regular multi-modal pattern convection can become preferred in some ranges of L_l^* and L_u^*, provided the wave vectors of such patterns are contained in certain subset of the wave vectors representing a linear combination of modulated lower and upper boundary temperatures. For non-resonant wavelength excitation case, three (two) dimensional solution in the form of multi-modal (rolls) pattern convection can be preferred, even if the boundary modulations are one (two) or two (one) dimensional, provided the wave lengths of the modulations are not too small. Heat transported by convection can be enhanced by boundary modulations in some ranges of L_l^* and L_u^*.

1. Introduction

The classical problem of Rayleigh-Bénard convection in a horizontal and symmetric layer with prescribed temperatures at the boundaries has been the subject of numerous investigations in the past. The linear theory was given in details by Chandrasekhar (1961). The notable subsequent nonlinear investigations of the problem were due to Malkus and Veronis (1958) and

Schlüter, Lortz and Busse (1965). Busse (1978) provides numerous references and excellent review on the subject. These and other investigations of such so-called perfect problem, which refers to the classical Rayleigh-Bénard convection with perfect isothermal boundaries, established, in particular, the following results: The linear problem is self-adjoint. The conduction state is unique for R below $R_c = 1707.8$ (for rigid boundaries). Here $R = \beta g \Delta T d^3/(k\nu)$ is the Rayleigh number, β is the coefficient of thermal expansion, g is the acceleration due to gravity, ΔT is the mean temperature difference across the layer, d is the depth of the layer, k is the thermal diffusivity, ν is the kinematic viscosity and R_c is the critical value of R below which there is no convection. The first bifurcation, which takes place at $R = R_c$, is thus supercritical, and the two-dimensional rolls with the critical wave number $\alpha_c = 3.12$ are the preferred mode of convection.

This paper studies the problem of weakly nonlinear thermal convection in a horizontal and symmetric layer with spatially modulated temperatures prescribed at both boundaries. This problem is an example of an imperfect bifurcation driven by imperfect heating and/or cooling (Tavantzis et al. 1978). There have been investigations of problems which are all relevant to the present investigation. Kelly and Pal (1976, 1978) and Pal and Kelly (1978) investigated two-dimensional thermal convection with one-dimensional spatially periodic boundary conditions. Tavantzis, Reiss and Matkowsky (1978) applied their theory of singular perturbations in a mathematical and systematic manner to the case of a bounded layer with a rather arbitrary one-dimensional variable temperature imposed on one boundary. Walton (1982, 1983) investigated the onset of thermal convection in a fluid layer of either slowly increasing depth or when the temperature difference between the horizontal boundaries is a monotonic function of a single horizontal variable. Krettenauer and Schumann (1989, 1992) carried out direct numerical simulation of thermal convection for the case where the lower surface height varied sinusoidally in one direction and for both laminar and turbulent flow regimes. More recently, Riahi (1993, henceforth referred to as R93) investigated the problem of preferred

pattern of convection in a porous layer when a spatially modulated temperature with amplitude L_l^* was prescribed at the lower boundary. He found, in particular, that, for the resonant wavelength excitation case, multi-modal pattern convection can be preferred in some range of L_l^*, provided the wave vectors of such pattern are contained in the set of wave vectors representing the spatially modulated lower wall temperature. The same method of analysis is applied in the present study to investigate nonlinear thermal convection in ordinary medium and its stability in the case of arbitrary Prandtl number p and when spatially modulated temperatures with amplitudes L_l^* and L_u^* were prescribed at the lower and upper boundaries, respectively. An important result of the present study is that the results based on the modulation on one boundary only can be quite misleading for the present problem since the results may be due to some unexpected linear combinations of the modulation modes on both boundaries. For example, in the case of one-dimensional modulation on only one boundary and for non-resonant wavelength excitation case, the preferred flow pattern is due to particular rectangular cells where the angle ω_b between two adjacent wave vectors of each cell is either

$$\omega_b = 2\cos^{-1}[\alpha^{(b)}/(2\alpha_c)] \quad \text{or} \quad 180° - \omega_b \tag{1.1}$$

and $\alpha^{(b)}$ denotes the magnitude of the lower boundary modulation wave vectors.

(R93), while in the case of one-dimensional modulations on both boundaries and for non-resonant wavelength excitation case, a multi-modal pattern convection ($N = 4$) can be preferred for some particular ranges of L_l^* and L_u^*, where 2N is the total number of wave vectors representing the flow pattern. A multi-modal pattern is defined as the one due to superposition of N rolls with distinct orientations. For even N a multi-modal pattern can also be defined as the one due to superposition of N/2 sets of rectangular patterns with distinct wave vectors. The result stated above for N = 4 is turned out to be due to superposition of two sets of particular

rectangular patterns. The angle between two adjacent wave vectors of one set of rectangular pattern is given by (1.1), while the angle ω_t between two adjacent wave vectors of another set of rectangular pattern is either

$$\omega_t = 2\cos^{-1}[\alpha^{(t)}/(2\alpha_c)] \quad \text{or} \quad 180° - \omega_t \tag{1.2}$$

and $\alpha^{(t)}$ denotes the magnitude of the upper boundary modulation wave vectors.

Hence the results of the present investigation can be unexpected and are important for cases where spatially modulated temperatures exist on both boundaries.

The present study assumes that convection is steady. This assumption is justified. For R just beyond R_c, steady solution prevails, since, to the leading order terms, the resulting linear system is identical to the corresponding classical one where steady solution is preferred (Chandrasekhar 1961). Yoo and Kim (1991)'s numerical investigation of two-dimensional convection with boundary modulation also indicates that steady convection is preferred for R up to values of order 10^5. The possibility for existence of non-stationary pattern due to vertical vorticity (Pismen 1987) is also ruled out here since the vertical vorticity for the present problem is found to be insignificant.

The general problem under consideration can have practical values in that one might want to modulate the temperature at the boundaries if the transport processes are enhanced or if the flow structure could be controlled. These aspects of the problem are the main motivation for the present study which is mostly concerned with the preferred convection pattern(s) and the heat transported by convection.

2. Formulation

We consider an infinite horizontal layer of fluid of average depth d and heated from below. The layer is bounded above and below by two rigid plane surfaces whose mean

temperatures are $\overline{T}_u$ and $\overline{T}_l$, respectively. We choose to scale the temperature T^* on the basis of $\Delta T = \overline{T}_l - \overline{T}_u$. It is convenient to introduce a cartesian system of coordinates, with the origin on the centerplane of the layer and with the z-coordinate in the vertical direction (opposite to the direction of the gravity force). We shall examine the effects of lower and upper boundary modulations at a fixed value of ΔT and represent the magnitudes of such variations relative to ΔT by δ_l and δ_u, respectively. It is assumed that $\delta_l < 0(1)$ and $\delta_u < 0(1)$. We define a temperature relative to the conduction state by

$$T^*(x,y,z,t) = \left(\frac{d}{2} - z\right)\frac{\Delta T}{d} + T(x,y,z,t), \tag{2.1}$$

where x and y are the horizontal variables and t is the time variable. It is convenient to use non-dimensional variables in which lengths, velocities, time and temperature are scaled respectively by $d, k/d, d^2/k$, and $\Delta T/R$. Under the Boussinesq approximation, which takes into account the significant buoyancy due to contribution of perturbation density to the gravity term in the momentum equation, the non-dimensional forms of the equations for momentum, heat and conservation of mass can be simplified by using the representation (Riahi 1985)

$$\underset{\sim}{u} = \Omega\phi \equiv \nabla x \nabla x (\underset{\sim}{z}\phi), \tag{2.2}$$

for the divergent free velocity vector $\underset{\sim}{u}$. Here $\underset{\sim}{z}$ represents a unit vector in the vertical direction. Taking the vertical component of the double curl of the momentum equation and using (2.2) in the heat equation yields the following governing equations:

$$\Delta_2\left(\nabla^4\phi - \theta - \frac{\partial}{\partial t}\nabla^2\phi\right) = p^{-1}\Omega \cdot [\Omega\phi \cdot \nabla(\Omega\phi)], \tag{2.3a}$$

$$\left(\nabla^2 - \frac{\partial}{\partial t}\right)\theta - R\Delta_2\phi = \Omega\phi \cdot \nabla\theta, \tag{2.3b}$$

where θ is the dimensionless T, $p = \nu/k$ is the Prandtl number, and Δ_2 is the horizontal Laplacian.

The boundary conditions for ϕ and θ are

$$\phi = \frac{\partial \phi}{\partial z} = 0 \quad \text{at} \quad z = \pm\frac{1}{2}, \tag{2.4a}$$

$$\theta = \delta_l R h_l(x,y) \quad \text{at} \quad z = -\frac{1}{2}, \tag{2.4b}$$

$$\theta = \delta_u R h_u(x,y) \quad \text{at} \quad z = \frac{1}{2}, \tag{2.4c}$$

where $h_l(x,y)$ and $h_u(x,y)$ are given spatially non-uniform function of x and y.

Alternative boundary conditions can be those of constant temperature corrugated rigid boundaries, where the conditions at the lower and upper boundaries for both ϕ and θ are prescribed at $z = -1/2 + \delta_l h_l$ and $z = 1/2 + \delta_u h_u$, respectively. Following appendix A in R93, it can be shown easily that the qualitative results of the present formulation, based on such lower and upper boundary conditions, do not differ from the corresponding results based on the boundary conditions given by (2.4).

3. The case of resonant wavelength excitation

Consider, first, the case of resonant wavelength excitation, where the wavelengths $\gamma_n^{(b)}$ and $\gamma_n^{(t)}$ of any n-th mode of the bottom and top boundary modulation, respectively, are equal to the critical wavelength $\gamma_c \equiv 2\pi/\alpha_c$ for the onset of classical convection. This case corresponds to the critical regime where $R \approx R_c, L_l^* = 0(\varepsilon^3)$ and $L_u^* = 0(\varepsilon^3)$ (Kelly and Pal 1978, R93), where ε is the amplitude of convection. We have designated the amplitudes of the non-uniform lower and upper boundary temperatures by $L_l^* = \delta_l L_l$ and $L_u^* = \delta_u L_u$, respectively, where it is assumed that $\varepsilon \ll 1, \delta_l = \delta_u = \varepsilon^3$, and L_l and L_u are order one quantities. Kelly and Pal (1976, 1978) demonstrated that this case corresponds to the critical range where L_l^* and L_u^* are of order ε^3. See Kelly and Pal (1976, 1978) for further details. We consider the following expansions for ϕ, θ and R in powers of ε

$$(\phi,\theta,R)=(0,0,R_0)+\varepsilon(\phi_1,\theta_1,R_1)+\varepsilon^2(\phi_2,\theta_2,R_2)+\ldots \tag{3.1}$$

Upon inserting (3.1) into (2.3)-(2.4) and disregarding the quadratic terms, we find the classical linear problem whose system is given by Schlüter et al. (1965) and by Riahi (1985). The general solution of this system can be written as

$$(\phi_1,\theta_1)=[f(z),g(z)]W(x,y), \tag{3.2}$$

where the function W has the representation

$$W(x,y)=\sum_{n=-N}^{N} C_n W_n \equiv \sum_{n=-N}^{N} C_n \exp(i\underset{\sim}{k}_n\cdot\underset{\sim}{r}), \tag{3.3}$$

and satisifes the relation

$$\Delta_2 W=-\alpha^2 W, <W^2>=1. \tag{3.4}$$

Here an angle bracket bracket indicates an average over the fluid layer, $\underset{\sim}{r}$ is the horizontal position vector, $i=\sqrt{-1}$, α is the horizontal wave number of the flow structure, N is a positive integer, and the horizontal wave vectors $\underset{\sim}{k}_n$ of the flow structure satisfy the properties

$$\underset{\sim}{k}_n\cdot\underset{\sim}{z}=0, \quad |\underset{\sim}{k}_n|=\alpha, \quad \underset{\sim}{k}_{-n}=-\underset{\sim}{k}_n. \tag{3.5}$$

The coefficients C_n satisfy the conditions

$$\sum_{n=-N}^{N} C_n C_n^*=1, \quad C_n^*=C_{-n}, \tag{3.6}$$

where the asterisk indicates the complex conjugate.

The complete solutions for the functions $f(z)$ and $g(z)$ introduced in (3.2) are given by Schlüter et al. (1965).

In the order ε^2, (2.3)-(2.4) lead to a system which is of the classical type (Schlüter et al. 1965, Riahi 1985), and the solution of this system is given in these references. Because of symmetric layer, $R_1=0$ (Riahi 1985).

Since the classical problem is self-adjoint, the solvability conditions for the equations of higher order in ε require us to define the following special solutions ϕ_{1n} and θ_{1n} of the linear system:

$$(\phi_{1n}, \theta_{1n}) = [f(z), g(z)]W_n. \tag{3.7}$$

In the order ε^3 system, the governing equations and the boundary conditions for ϕ_3 are the same as the corresponding ones for the classical problem (Schlüter et al., 1965, Riahi 1985), while the temperature boundary conditions become

$$\theta_3 = R_0 h_l \quad \text{at} \quad z = -\frac{1}{2}, \tag{3.8a}$$

$$\theta_3 = R_0 h_u \quad \text{at} \quad z = \frac{1}{2}. \tag{3.8b}$$

The fractions h_l and h_u given in (3.8) are actually assumed to have the following arbitrary representation

$$h_l(x,y) = \sum_{n=-N^{(b)}}^{N^{(b)}} L_l C_n^{(b)} W_n^{(b)} \equiv \sum_{n=-N^{(b)}}^{N^{(b)}} L_l C_n^{(b)} \exp(i\underset{\sim}{k}_n^{(b)} \cdot \underset{\sim}{r}), \tag{3.9a}$$

$$h_u(x,y) = \sum_{n=-N^{(t)}}^{N^{(t)}} L_u C_n^{(t)} W_n^{(t)} \equiv \sum_{n=-N^{(t)}}^{N^{(t)}} L_u C_n^{(t)} \exp(i\underset{\sim}{k}_n^{(t)} \cdot \underset{\sim}{r}), \tag{3.9b}$$

where L_l and L_u are constants, $N^{(b)}$ and $N^{(t)}$ are positive integers which may tend to infinity, and the horizontal wave vectors $\underset{\sim}{k}_n^{(b)}$ and $\underset{\sim}{k}_n^{(t)}$ satisfy the properties

$$\underset{\sim}{k}_n^{(b)} \cdot \underset{\sim}{z} = 0, \quad |\underset{\sim}{k}_n^{(b)}| = \alpha_n^{(b)} \equiv 2\pi/\gamma_n^{(b)}, \quad \underset{\sim}{k}_{-n}^{(b)} = -\underset{\sim}{k}_n^{(b)}, \tag{3.10a}$$

$$\underset{\sim}{k}_n^{(t)} \cdot \underset{\sim}{z} = 0, \quad |\underset{\sim}{k}_n^{(t)}| = \alpha_n^{(t)} \equiv 2\pi/\gamma_n^{(t)}, \quad \underset{\sim}{k}_{-n}^{(t)} = -\underset{\sim}{k}_n^{(t)}, \tag{3.10b}$$

The coefficients $C_n^{(b)}$ and $C_n^{(t)}$ satisfy the conditions

$$\sum_{n=-N^{(b)}}^{N^{(b)}} C_n^{(b)} C^{*(b)}_n = 1, \quad C^{*(b)}_n = C^{(b)}_{-n}, \tag{3.11a}$$

$$\sum_{n=-N^{(t)}}^{N^{(t)}} C_n^{(t)} C^{*(t)}_n = 1, \quad C^{*(t)}_n = C^{(t)}_{-n}. \tag{3.11b}$$

We shall assume that $\alpha_n^{(b)} = \alpha_n^{(t)} = \alpha_c = 3.12$. In general, $\alpha_n^{(b)}$ and $\alpha_n^{(t)}$ are not all the same as α_c for different n. Major portions of these later cases will be considered later in section 4, while the rest will be discussed in section 5. Multiplying (2.3a) in the order ε^3 by ϕ^*_{1n}, (2.3b) in the order ε^3 by $R_c^{-1}\theta^*_{1n}$, adding and averaging over the whole layer and using (2.4a) in the order ε^3 and (3.8) yields a system of $2N+1$ equations for R_2 and C_n ($n = -N, \ldots, -1, 1, \ldots, N$). Using the procedure discussed in Riahi (1985) and in R93, this system can be simplified into the following form:

$$F_0(R_2^{(N)} - R_{2C}^{(N)}) \cdot C_n = -F_1[L_l \sum_{m=-N^{(b)}}^{N^{(b)}} C_m^{(b)} < W_n^* W_m^{(b)} > +$$

$$L_u \sum_{m=-N^{(t)}}^{N^{(t)}} C_m^{(t)} < W_n^* W_m^{(t)} >],$$

$$n = (-N, \ldots, -1, 1, \ldots, N) \tag{3.12}$$

where $F_0 = \alpha_c^2 < fg >$, $F_1 = \partial g / \partial z \mid_{z=-1/2}$ and $R_2^{(N)}$ and $R_{2C}^{(N)}$ denotes the present and the classical expressions for R_2 (Riahi 1985) in the case where the associated flow pattern contains a total of 2N wave vectors (see (3.3)). In deriving (3.12), we use the result that F_1 equals $-\frac{\partial g}{\partial z} \mid_{z=1/2}$ (Schlüter et al. 1965). Both F_0 and F_1 as well as $R_{2C}^{(N)}$ are positive (Schlüter et al. 1965, Riahi 1985). Using the approximate relationship

$$H = < \theta (z \cdot u) > \approx \varepsilon^2 \alpha_c^2 < fg > \approx F_0 (R - R_c) / R_2^{(N)}, \tag{3.13}$$

For the heat transported by convection, we can determine from (3.12)-(3.13) the functional relationship between H and the parameters P, L_l and L_u for various flow and boundary modulation patterns.

To distinguish the physically realizable solution(s) among all possible steady solutions, the stability of ϕ, θ with respect to arbitrary three dimensional disturbances $\tilde{\phi}, \tilde{\theta}$ are investigated. The equations and the boundary conditions for the time dependent disturbances with addition of a time dependence of the form $\exp(\sigma t)$ are of the same classical forms given by Schlüter et al. (1965) and Riahi (1985) and will not be repeated here. When (3.1) is used in this system it becomes evident that the stability system can be solved by an expansion of the form

$$(\tilde{\phi}, \tilde{\theta}, \sigma) = (\tilde{\phi}_1, \tilde{\theta}_1, \sigma_0) + \varepsilon(\tilde{\phi}_2, \tilde{\theta}_2, \sigma_1) + \ldots \tag{3.14}$$

The solutions to the stability problem can be obtained in direct analogy to that discussed by Riahi (1985) for the classical problem ($\delta_l = \delta_u = 0$ case). The solvability conditions in the orders $\varepsilon^n (n = 0, 1, 2)$ lead to the following results for the growth rate of the most critical disturbances:

$$\sigma_0 = \sigma_1 = 0, \quad (\sigma_2 - \sigma_{2C}) < g^2 > = (R_2^{(N)} - R_{2C}^{(N)}) F_0, \tag{3.15}$$

where σ_{2C} denotes the classical expression for σ_2 given by Riahi (1985).

Using (3.12)-(3.13), (3.15) and the results given by Riahi (1985) for $R_{2C}^{(N)}$ and σ_{2C}, we obtain the following non-trivial results: for sufficiently large and positive values of L_l and L_u, $R_2^{(N)} < 0$ and, thus, the corresponding solution is subcritical ($R < R_c$). For sufficiently large and positive values of L_l and L_u, there may be more than one stable solution. However, the preferred solution corresponds to the one for which R is minimum. The effects of the surface modulation on the flow structures and on the heat flux are independent of the location of the surface. For some ranges of L_l and L_u, the heat flux is enhanced, while for some other ranges of L_l and L_u, the heat flow is reduced.

The averaged product terms in the right hand side of (3.12) can be non-zero only if, at least, one of the wave vectors $\underset{\sim}{k}_n$ is in the direction of $\underset{\sim}{k}_m^{(b)}$ or $\underset{\sim}{k}_m^{(t)}$. If none of the wave vectors $\underset{\sim}{k}_n$ are along any of the boundary modulation wave vectors $\underset{\sim}{k}_m^{(b)}$ and $\underset{\sim}{k}_m^{(t)}$, or if $L_l = -L_u$ and $\underset{\sim}{k}_m^{(b)} = \underset{\sim}{k}_m^{(t)}$,

then the right hand side terms in (3.12) and (3.15) are zero, $R_2^{(N)} = R_{2c}^{(N)}, \sigma_2 = \sigma_{2c}$ and the preferred flow pattern is the same as in the classical unmodulated problem (Riahi 1985), where two-dimensional rolls are preferred and orientational degeneracy of the rolls solutions persists.

In order to derive some relatively general results based on some special examples and for effective boundary modulations, we shall assume that at least some wave vectors $\underset{\sim}{k}_n$ are along the boundary modulation wave vectors and restrict our analysis to the cases where

$$c_n^{(b)} = (2N^{(b)})^{-1/2}, \quad c_n^{(t)} = (2N^{(t)})^{-1/2}, \tag{3.16a,b}$$

$$L_l > 0, \quad L_u > 0. \tag{3.16c,d}$$

The assumptions given by (3.16a,b), which reduce the complexity of the problem considerably, satisfy (3.11) and correspond to the so-called regular or semi-regular modulation patterns (R93). The conditions (3.16c,d) then imply that only the most significant effects of the boundary modulations are considered here (R93). The assumptions (3.16) are also supported by our present finding that only cases with $L_l c_n^{(b)} < 0$ or $L_u c_n^{(t)} < 0$ correspond to values of R smaller than the corresponding values for cases with $L_l c_n^{(b)} > 0$ or $L_u c_n^{(t)} > 0$, respectively.

Let us now consider the following few specific examples in order to illustrate the interesting and often surprising inter-relations between the boundary modulation pattern and the subsequence preferred flow pattern:

Example 1. $N^{(b)} = N^{(t)} = 1$.

For $L_l \neq L_u$ and $\underset{\sim}{k}_m^{(b)}$ inclined with respect to $\underset{\sim}{k}_m^{(t)}$, we find from (3.12) and (3.15) that two-dimensional rolls are preferred and that

$$(R_2^{(1)} - R_{2C}^{(1)})(F_0/F_1) = \begin{cases} -L_l & \text{for} \quad L_l > L_u, \\ -L_u & \text{for} \quad L_u > L_l, \end{cases} \tag{3.17a}$$

$$\sigma_2 - \sigma_{2C} < 0. \tag{3.17b}$$

The expression for σ_{2C} is negative only for two-dimensional rolls convection (Riahi 1985). Any other solutions (three-dimensional solutions) are not allowed by the nonlinear system in the case $L_l \neq L_u$.

The results discussed above indicate that all the two-dimensional rolls solutions parallel to any direction are stable. However, rolls parallel to $\underset{\sim}{k}_m^{(b)}$ or $\underset{\sim}{k}_m^{(t)}$ have smaller R if $L_l > L_u$ or $L_u > L_l$, respectively, as evidenced from (3.17), and are, therefore, preferred. For $L_l = L_u \equiv L$ and $\underset{\sim}{k}_m^{(b)}$ inclined with respect to $\underset{\sim}{k}_m^{(t)}$, two-dimensional rolls parallel to either $\underset{\sim}{k}_1^{(b)}$ or $\underset{\sim}{k}_1^{(t)}$ are stable, correspond to the same R, and they satisfy (3.17). For three dimensional convection in the form of rectangular cells whose wave vectors coincide with $\underset{\sim}{k}_m^{(b)}$ and $\underset{\sim}{k}_m^{(t)}(m = -1, 1)$, we find (3.17b) and the following expression for $R_2^{(2)}$

$$(R_2^{(2)} - R_{2C}^{(2)})\,(F_0/F_1) = -\sqrt{2}\,L_l. \tag{3.18}$$

No other three dimensional solutions are possible. The expression (3.17a) for $R_2^{(1)}$ is less than (greater than) the expression (3.18) for $R_2^{(2)}$ if L is less than (greater than) l_0, where

$$l_0 = (R_{2C}^{(2)} - R_{2C}^{(1)})\,F_0/[(\sqrt{2}-1)\cdot F_1].$$

Hence the preferred flow pattern, which corresponds to the minimum R, is that due to two-dimensional rolls along either $\underset{\sim}{k}_1^{(b)}$ or $\underset{\sim}{k}_1^{(t)}$ for $L < l_0$, while rectangular pattern convection is preferred for $L > l_0$. The wave vectors for these rectangular cells coincide with those due to boundary modulations. For $\underset{\sim}{k}_m^{(b)}$ along $\underset{\sim}{k}_m^{(t)}$, no such three-dimensional pattern is possible. Two dimensional rolls along $\underset{\sim}{k}_m^{(b)}$ are then preferred and (3.12) becomes

$$(R_2^{(1)} - R_{2C}^{(1)})\,(F_0/F_1) = -2L_l. \tag{3.19}$$

In this example we encountered a situation where two different sets of rolls correspond to the same minimum R for particular ranges of the modulation amplitudes. The realizable flow pattern is then the one due to one of these two sets which is under a favorable initial condition such as an initial disturbance roll along such set of rolls.

Example 2. $N^{(b)}=2$ and $N^{(t)}=1$. For $L_l=\sqrt{2}\,L_u$ and $\underset{\sim}{k}_m^{(b)}=\underset{\sim}{k}_m^{(t)}$ say $(m=-1,1)$, the only possible stable solutions are due to rolls, and two-dimensional rolls along $\underset{\sim}{k}_2^{(b)}$ are preferred. For $L_l\neq\sqrt{2}\,L_u$ and $\underset{\sim}{k}_m^{(b)}$ inclined with respect to $\underset{\sim}{k}_m^{(t)}$, we find from (3.12) and (3.15) that two-dimensional rolls can be stable and that

$$(R_2^{(1)}-R_{2C}^{(1)})(F_0/F_1) = \begin{cases} -L_l/\sqrt{2} & \text{for } L_l > \sqrt{2}\,L_u, \\ -L_u & \text{for } L_l < \sqrt{2}\,L_u \end{cases} \tag{3.20}$$

As evidenced from (3.20), rolls along $\underset{\sim}{k}_m^{(b)}$ are preferred over rolls along $\underset{\sim}{k}_m^{(t)}$ for $L_l/\sqrt{2}>L_u$, while rolls along $\underset{\sim}{k}_m^{(t)}$ are preferred over rolls along $\underset{\sim}{k}_m^{(b)}$ for $L_u>L_l/\sqrt{2}$. Rectangular pattern with wave vectors along $\underset{\sim}{k}_m^{(b)}$ can also be stable whose expression for $R_2^{(2)}$ is in the form

$$(R_2^{(2)}-R_{2C}^{(2)})(F_0/F_1)=-L_l. \tag{3.21}$$

Of course, the flow pattern, which is actually preferred, has the smallest value of R_2. Using (3.20)-(3.21), we find that rolls along $\underset{\sim}{k}_m^{(b)}$ are preferred for $L_l<\sqrt{2}\,l_0$ (if $L_l/\sqrt{2}>L_u$), while rolls along $\underset{\sim}{k}_m^{(t)}$ are preferred for $(L_l-L_u)<(\sqrt{2}-1)l_0$ (if $L_l/\sqrt{2}<L_u$). On the other hand, rectangular cells along $\underset{\sim}{k}_m^{(b)}$ are preferred for either $L_l>\sqrt{2}\,l_0$(if$L_l>\sqrt{2}\,L_u$) or $L_l-L_u>(\sqrt{2}-1)l_0$(if$L_l<\sqrt{2}\,L_u$). For $L_l=\sqrt{2}\,L_u$ and for the case where $\underset{\sim}{k}_m^{(b)}$ are inclined with respect to $\underset{\sim}{k}_m^{(t)}$, rolls parallel to either $\underset{\sim}{k}_m^{(b)}$ or $\underset{\sim}{k}_m^{(t)}$ are stable, and they satisfy (3.20). For rectangular cells, whose wave vectors coincide either with $\underset{\sim}{k}_m^{(b)}$ or with $\underset{\sim}{k}_m^{(t)}$ and $\underset{\sim}{k}_m^{(b)}$, we find the expression (3.21) for $R_2^{(2)}$. The expression (3.20) for $R_2^{(1)}$ is less than (greater than) the expression

(3.21) for $R_2^{(2)}$ if L_l is less than (greater than) l_1, where $l_1 = \sqrt{2}\, l_0$. For 6-sided polygonal (superposition of three sets of inclined rolls) cells, whose wave vectors coincide with $\underset{\sim}{k}_m^{(b)}$ and $\underset{\sim}{k}_m^{(t)}$, we find

$$(R_2^{(3)} - R_{2C}^{(3)})(F_0/F_1) = -\sqrt{3}L_l/\sqrt{2}. \tag{3.22}$$

The expression (3.21) for $R_2^{(2)}$ is less than (greater than) the expression (3.22) for $R_2^{(3)}$ if L_l is less than (greater than) l_2, where

$$l_2 = (R_{2C}^{(3)} - R_{2C}^{(2)})F_0 \cdot \sqrt{2}/[F_1(\sqrt{3}-\sqrt{2})].$$

Hence, two-dimensional rolls (3 sets) are preferred for $L_l < l_1$, rectangular patterns (3 sets) are preferred for $l_1 < L_l < l_2$ and 6-sided polygonal pattern convection (1 set) is preferred for $l_2 < L_l$. For $L_l = \sqrt{2}L_u$ and for the case where $\underset{\sim}{k}_m^{(b)}(m = 1\text{or}2)$ is along $\underset{\sim}{k}_m^{(t)}$, no such three-dimensional patterns is possible. Two-dimensional rolls along $\underset{\sim}{k}_m^{(t)}$ are then preferred and (3.19) follows.

In this example we also have multiple solutions corresponding to the same minimum R which occur in some particular ranges of L_l and L_u. As was discussed in the previous example, the preferred solution is then due to initial condition.

Example 3. $N^{(b)} = N^{(t)} = 2$. Following the procedure discussed in the above two examples, we find the following results. For $L_l \neq L_u$ and for the case where $\underset{\sim}{k}_m^{(b)}$ are inclined with respect to $\underset{\sim}{k}_m^{(t)}$, then two-dimensional rolls along $\underset{\sim}{k}_1^{(b)}$ (or $\underset{\sim}{k}_{-1}^{(b)}$) or along $\underset{\sim}{k}_2^{(b)}$ (or $\underset{\sim}{k}_{-2}^{(b)}$) are preferred for $l_0 > L_l > L_u$, while two-dimensional rolls along $\underset{\sim}{k}_1^{(t)}$ (or $\underset{\sim}{k}_{-1}^{(t)}$) or along $\underset{\sim}{k}_2^{(t)}$ (or $\underset{\sim}{k}_{-2}^{(t)}$) are preferred for $l_0 > L_u > L_l$. Rectangular pattern with wave vectors along $\underset{\sim}{k}_m^{(b)}$ are preferred for $L_l > L_u$ and $L_l > l_0$, while such pattern with wave vectors along $\underset{\sim}{k}_m^{(t)}$ are preferred for $L_l < L_u$ and $L_u > l_0$. For $L_l = L_u$ and for the case where $\underset{\sim}{k}_m^{(b)}$ are all inclined with respect to $\underset{\sim}{k}_m^{(t)}$, we find that for L_l in the ranges $0 < L_l < l_1, l_1 < L_l < l_2, l_2 < L_l < l_3$ and $l_3 < L_l$, two-dimensional rolls, rectangular pattern, 6-sided polygonal pattern and multi-modal pattern (N = 4) are preferred, respectively. Here

$$l_3 = (R_{2C}^{(4)} - R_{2C}^{(3)})F_0\sqrt{2}/[F_1(2-\sqrt{3})].$$

We have assumed that $R_{2C}^{(i+1)} > R_{2C}^{(i)}$ and $R_{2C}^{(j+2)} - 2R_{2C}^{(j+1)} + R_{2C}^{(j)} > 0$ for $i, j = 1, 2, \ldots$. These assumptions appear to be valid, at least for $i = 1, 2$ and $j = 1$, in the cases of regular patterns due to rolls, squares and hexagons (Schlüter et al. 1965, Riahi 1985). However, we have not been able to find a rigorous proof for arbitrary i and j. We also assumed that $C_n = 1/\sqrt{2N}$ which satisfies the condition (3.6) and reduces the complexity of the problem particularly for $N > 2$. For the case where one of the wave vectors $\underset{\sim}{k}_m^{(b)}$, say $\underset{\sim}{k}_1^{(b)}$, is along one of the wave vectors $\underset{\sim}{k}_m^{(t)}$, then two-dimensional rolls along $\underset{\sim}{k}_1^{(b)}$ are preferred and (3.18) follows. For the case where $\underset{\sim}{k}_m^{(b)}$ are along $\underset{\sim}{k}_m^{(t)} (m = -2, \ldots, 2)$, we find that for $L_l + L_u$ in the ranges of $0 < L_l + L_u < l_1$ and $l_1 < L_l + L_u$, two-dimensional rolls and rectangular pattern are preferred, respectively.

The three examples presented above indicate a general theory for arbitrary $N^{(b)}$ and $N^{(t)}$ and for the case where the wave vectors of the flow coincide with a subset of wave vectors of the upper and lower boundary modulations. Such theory, to be discussed below in the following 3 parts, is consistent with the results for $N^{(b)}, N^{(t)} = 1, 2$. However, we have not been able to find a rigorous proof for arbitrary $N^{(b)}$ and $N^{(t)}$. Consider the case where $C_n = 1/\sqrt{2N}$. This case satisfies the condition (3.6) and reduces the complexity of the problem considerably. I) For $(L_l/L_u)^2 \neq N^{(b)}/N^{(t)}$ and for the case where none of $\underset{\sim}{k}_m^{(b)}$ are along any of $\underset{\sim}{k}_m^{(t)}$, then the lower (upper) boundary modulation dominates over the upper (lower) boundary modulation for $(L_l/L_u)^2 > N^{(b)}/N^{(t)}[(L_l/L_u)^2 < N^{(b)}/N^{(t)}]$, at least for the same flow structures under these conditions. There exist positive constants l_i and u_j $(i = 1, \ldots, N^{(b)} - 1; j = 1, \ldots, N^{(t)} - 1)$ such that $l_i < l_{i+1}$ and $u_j < u_{j+1}$ for all i and j. For $l_{j-1} < L_l < l_j$, multi-modal (N = j) pattern convection is preferred only if the wave vectors of such pattern are participating in the expression (3.9a) for $h_l(x, y)$. For $L_l > l_m, m = N^{(b)} - 1$, multi-modal $(N = N^{(b)})$ pattern convection is preferred only if the wave vectors of such pattern are participating in the expression for h_l. The following expression for l_j

is obtained by equating the expressions for $R_2^{(j)}$ and $R_2^{(j+1)}$ derived from (3.12)

$$l_j = F_0[R_{2C}^{(j+1)} - R_{2C}^{(j)}]\,(N^{(b)})^{1/2}/[F_1(\sqrt{j+1}-\sqrt{j})].$$

Similarly, for $u_{j-1} < L_u < u_j$, multi-modal ($N = j$) pattern convection is preferred only if the wave vectors of such pattern are participating in the expression (3.9b) for $h_u(x, y)$. For $L_u > u_m, m = N^{(t)} - 1$, multi-modal ($N = N^{(t)}$) pattern convection is preferred only if the wave vectors of such pattern are participating in the expression for h_u. The expression for u_j is the same as that for l_j, provided $N^{(b)}$ is replaced by $N^{(t)}$. To determine the actual preferred flow pattern, we need to examine the condition

$$R_2^{(j)}(\text{for} L_u = 0) < R_2^{(s)}(\text{for} L_l = 0). \tag{3.23}$$

Using (3.12) and (3.23), we find that for L_u and L_l in the range

$$L_u\sqrt{\frac{S}{N^{(t)}}} - L_l\sqrt{\frac{j}{N^{(b)}}} < (R_{2C}^{(s)} - R_{2C}^{(j)})\,(F_0/F_1), \tag{3.24}$$

then the multi-modal ($N = j$) pattern convection whose wave vectors participating in the expression for h_l is preferred over the multi-modal ($N = S$) pattern convection whose wave vectors participating in the expression for h_u. If the left hand side of (3.24) is bigger than the right hand side of (3.24), then the opposite is true. In practice, one has to check (3.24) for each S ($S = 1, \ldots, N^{(t)} - 1$) and each j ($j = 1, \ldots, N^{(b)} - 1$) given the ranges $l_{j-1} < L_l < l_j$ and $u_{s-1} < L_u < u_s$.

II) For $(L_l/L_u)^2 = N^{(b)}/N^{(t)}$ and for the case where none of $\underset{\sim}{k}_m^{(b)}$ are along any of $\underset{\sim}{k}_m^{(t)}$, then a simple re-arrangement can convert the two separate expression in the right hand side of (3.12) into one single expression with the range of the subscript m from $-(N^{(b)} + N^{(t)})$ to $(N^{(b)} + N^{(t)})$. The result is then equivalent to the case of modulation on one boundary only. There exists positive constants $l_j (j = 1, \ldots, N^{(b)} + N^{(t)} - 1)$ (defined in part I before) such that multi-modal ($N = j$) pattern convection is preferred in the range $l_{j-1} < L_l < l_j$ only if the wave vectors of such pattern are participating in the expression $h_l + h_u$. For $L_l > l_m, m = N^{(b)} + N^{(t)} - 1$, multi-modal

($N = N^{(b)} + N^{(t)}$) pattern convection is preferred only if the wave vectors of such pattern are the same as those for $h_l + h_u$. III) For the case where M number of wave vectors $\underset{\sim}{k}_m^{(b)}$ coincide with M number of wave vectors $\underset{\sim}{k}_m^{(t)}$ ($0 < M \leq \min(N^{(b)}, N^{(t)})$), then the total modes representing the boundary modulations can be divided into the following 3 sets: Set 1 of M modes, with coefficients $L_l/\sqrt{N^{(b)}} + L_u/\sqrt{N^{(t)}}$, which are contained in both h_l and h_u, set 2 of $(N^{(b)} - M)$ modes, with coefficients $L_l/\sqrt{N^{(b)}}$, which are contained in h_l only and set 3 of $(N^{(t)} - M)$ modes, with coefficients $L_u/\sqrt{N^{(t)}}$, which are contained in h_u only. Hence, this case is then a generalization of part I described before. There exist positive constants l_i, u_j and $v_n (i = 1, \ldots, N^{(b)} - M - 1;$ $j = 1, \ldots, N^{(t)} - M - 1; n = 1, \ldots, M - 1)$ such that $l_i < l_{i+1}, u_j < u_{j+1}$ and $v_n < v_{n+1}$ for all i, j and n. For $l_{j-1} < L_l < l_j$, multi-modal ($N = j$) pattern convection is preferred only if all $\underset{\sim}{k}_n$ are contained in the set 2. For $L_l > l_m, m = N^{(b)} - M - 1$, multi-modal ($N = N^{(b)} - M$) pattern convection is preferred only if all $\underset{\sim}{k}_n$ coincide with those in set 2. The expression for l_j is already given in part I of the general theory. Similarly, for $u_{j-1} < L_u < u_j$, multi-modal ($N = j$) pattern convection is preferred only if all $\underset{\sim}{k}_n$ are contained in the set 3. For $L_u > u_m, m = N^{(t)} - M - 1$, multi-modal ($N = N^{(t)} - M$) pattern convection is preferred only if all $\underset{\sim}{k}_n$ coincide with those in set 3. The expression for u_j is already described in part I. Likewise, for $v_{j-1} < L_l/\sqrt{N^{(b)}} + L_u/\sqrt{N^{(t)}} < v_j$, multi-modal ($N = j$) pattern convection is preferred only if all $\underset{\sim}{k}_n$ are contained in the set 1. For $L_l/\sqrt{N^{(b)}} + L_u/\sqrt{N^{(t)}} > v_m, m = M - 1$, multi-modal ($N = M$) pattern convection is preferred only if all $\underset{\sim}{k}_n$ coincide with those in set 1. Similar to the procedure used to determine l_j, v_j can be found. It is of the same form to that of l_j, provided $l_j/\sqrt{N^{(b)}}$ is replaced by v_j. To determine the actual preferred flow pattern, we need to apply a procedure similar to that described in part I. Briefly, one needs to compare $R_2^{(j)}$ for the three sets of modes which lead to certain range(s) for L_l and L_u under which $R_2^{(j)}$, for particular set of the modes, is smallest. The flow pattern corresponding to such $R_2^{(j)}$ is then the preferred one in such ranges for L_l and L_u as was discussed in part I.

In cases where more than one flow pattern corresponds to the same minimum R, the realizable pattern is the one of these patterns which is due to some initial conditions. Diagram 1 provides types of the flow patterns that are preferred under certain ranges of the modulation amplitudes and under certain orientations of the modulation wave vectors.

4. The case of non-resonant wavelength excitation

This case corresponds to the critical regime where $R \approx R_c$ and it turns out, as was shown in R93, that non-trivial results are due to cases where $0(\varepsilon^2) \le \delta_u < 0(\varepsilon)$ and/or $0(\varepsilon^2) \le \delta_l < 0(\varepsilon)$.

We shall assume that $L_l^* = 0(L_u^*)$ since we are interested in cases where modulations on both boundaries can be significant. Hence, we set $\delta_l = \delta_u \equiv \delta$. Following Pal and Kelly (1978), we consider the following double expansions for ϕ, θ and R in powers of ε and δ:

$$(\phi, \theta, R) = \sum_{m=0} \sum_{n=0} \varepsilon^m \delta^n (\phi_{mn}, \theta_{mn}, R_{mn});$$

$$\phi_{00} = \theta_{00} = 0. \tag{4.1}$$

Upon inserting (4.1) into (2.3)-(2.4) and disregarding the quadratic terms, we find the linear problem whose order $\varepsilon^1\delta^0$ system is the classical linear system with solution of the form (3.2), provided that ϕ_1 and θ_1 are replaced, respectively, by ϕ_{10} and θ_{10}. The order $\varepsilon^0\delta^1$ system of the linear problem is of the form given by (A.1) in appendix.

The general solutions of the system (A.1) can be written as

$$(\phi_{01}, \theta_{01}) = \sum_{n=-N^{(b)}}^{N^{(b)}} L_l[F_{ln}(z), G_{ln}(z)] C_n^{(b)} W_n^{(b)} +$$

$$\sum_{n=-N^{(t)}}^{N^{(t)}} L_u[F_{un}(z), G_{un}(z)] C_n^{(t)} W_n^{(t)}, \tag{4.2}$$

where F_{ln}, G_{ln}, F_{un} and G_{un} are the solution of the system (A.2) given in the appendix. The solution to (A.2) is given by (A.3) in the appendix.

Similar to the result found by Pal and Kelly (1978) and in R93, the results (A.2)-(A.3) in the appendix indicate that the double series expansions procedure of this section breaks down for either $\alpha_n^{(b)} = \alpha_c$ or $\alpha_n^{(t)} = \alpha_c$ since F_{ln} and G_{ln} or F_{un} and G_{un} become unbounded. Hence, our method of solution here is strictly valid for $\alpha_n^{(b)} \neq \alpha_c$ and $\alpha_n^{(t)} \neq \alpha_c$.

Some preliminary investigations indicated that the trivial result that the boundary modulation(s) controls the flow patterns will be followed if $\delta \geq 0(\varepsilon)$. Hence significant results are due to cases where $\delta < 0(\varepsilon)$. However, consideration of the series expansion for R given in (4.1) indicates that the present weak imperfection can lead to significant results only if

$$R_{01}\delta \gg R_{20}\varepsilon^2,$$

where $R_{20} = R_{2c}$ is the classical expression for R_2 introduced in (3.12). Hence

$$0(\varepsilon^2) < \delta < 0(\varepsilon). \tag{4.3}$$

This result implies the need for the expression for R_{01} which is found by applying the solvability conditions for the order $\varepsilon\delta$ system of the nonlinear problem. It is

$$R_{01}\alpha_c^2 < \theta_{10n}\phi_{10} > = < \theta_{10n}(\Omega\phi_{10} \cdot \nabla\theta_{01} + \Omega\phi_{01} \cdot \nabla\theta_{10}) > +$$

$$P^{-1}R_c < \phi_{10n}\Omega \cdot (\Omega\phi_{10} \cdot \nabla\Omega\phi_{01} + \Omega\phi_{01} \cdot \nabla\Omega\phi_{10}) >, \tag{4.4}$$

where $(\theta_{10n}, \phi_{10n})$ have the same expressions as (θ_{1n}, ϕ_{1n}) introduced in (3.7). Using the classical solution for f and g introduced in (3.2) (Riahi 1985), (4.2) and (A.1)-(A.3) in the appendix, (4.4) can be simplified into the following form

$$R_{01}C_n^* \sum_{m,p} [L_l S_{mp}^{(b)} C_m C_p^{(b)} < W_n W_m W_p^{(b)} > +$$

$$L_u S_{mp}^{(t)} C_m C_p^{(t)} < W_n W_m W_p^{(t)} >], \tag{4.5}$$

where the expressions for the coefficients $S_{mp}^{(b)}$ and $S_{mp}^{(t)}$, which are functions of $(P, \alpha_p^{(b)}, \phi_{mp}^{(b)})$ and $(P, \alpha_p^{(t)}, \phi_{mp}^{(t)})$, respectively, are given in the appendix and

$$\phi_{mp}^{(b)} = (\underset{\sim}{k}_m \cdot \underset{\sim}{k}_p^{(b)})/(\alpha_c \alpha_p^{(b)}), \quad \phi_{mp}^{(t)} = (\underset{\sim}{k}_m \cdot \underset{\sim}{k}_p^{(t)})/(\alpha_c \alpha_p^{(t)}).$$

It can be seen from (4.5) that R_{01} can be non-zero only if

$$\underset{\sim}{k}_n + \underset{\sim}{k}_m + \underset{\sim}{k}_p^{(b)} = 0 \tag{4.6a}$$

or

$$\underset{\sim}{k}_n + \underset{\sim}{k}_m + \underset{\sim}{k}_p^{(t)} = 0 \tag{4.6b}$$

For at least some m and p. Using (3.5) and (3.10), we find that the conditions (4.6a) or (4.6b) can not be satisfied if

$$\alpha_p^{(b)} > 2\alpha_c \tag{4.7a}$$

or

$$\alpha_p^{(t)} > 2\alpha_c. \tag{4.7b}$$

If the conditions (4.7a) and (4.7b) are satisfied for all possible p, then $R_{01} = 0$ and the dominant effects can be isolated by considering the terms

$$R_{02}\delta^2 + R_{11}\varepsilon\delta + R_{20}\varepsilon^2$$

in the series expansion (4.1) for R. It is seen from the above expression that if $0(\varepsilon^2) \le \delta^2 \ll 0(1)$, then $0(\varepsilon) \le \delta \ll 1$ and the trivial result that the boundary modulation removes the pattern degeneracy at the linear level follows. On the other hand, if $\delta^2 \ll 0(\varepsilon^2)$, then the R_{20} term dominates over the other terms in the above expression implying negligible imperfection effect. Hence, significant results due to significant boundary modulations exist only if

$$\alpha_p^{(b)} \le 2\alpha_c \text{ or } \alpha_p^{(t)} \le 2\alpha_c \tag{4.8a,b}$$

for at least some p.

We shall assume that the conditions (4.8a,b) are valid. Note that the expressions for R_{01} given by (4.5) can always be negative for the boundary modulations represented either by the functions h_l and h_u or by the functions $(-h_l)$ and $(-h_u)$, respectively. For the cases where (4.8) hold, we actually evaluated the expression (4.5) for R_{01} and found that $R_{01} < 0$ for $L_l C_p^{(b)} > 0$ and $L_u C_p^{(t)} > 0$, respectively, while $R_{01} > 0$ for $L_l C_p^{(b)} < 0$ and $L_u C_p^{(t)} < 0$, respectively. Hence subcritical instability ($R < R_c$) is possible and is preferred over supercritical case ($R > R_c$).

In order to derive some relatively general results based on some special examples and for effective boundary modulations, we shall assume that at least some wave vectors $\underset{\sim}{k}_n$ are along the boundary modulation wave vectors and restrict our analysis here to the cases where (3.16) and

$$\alpha_p^{(b)} \equiv \alpha^{(b)}, \quad \alpha_p^{(t)} \equiv \alpha^{(t)} \qquad (4.9a,b)$$

hold, where $\alpha^{(b)}$ and $\alpha^{(t)}$ have fixed values satisfying (4.8). The assumptions (3.16) and (4.9) reduce the complexity of the problem considerably and enable to obtain some relatively general results for cases where the boundary modulation effects can be significant.

Let us now consider the following few specific examples in order to illustrate the non-trivial and often surprising inter-relation between the boundary modulations patterns and the subsequent preferred flow pattern:

Example 1. $N^{(b)} = N^{(t)} = 1$ and $\alpha^{(b)} = \alpha^{(t)} = 2\alpha_c$.

The expression in the right hand side of (4.5) can be non-zero only if

$$\phi_{mp}^{(b)} = -1 \text{ or } \quad \phi_{mp}^{(t)} = -1.$$

This result implies that the possible preferred solution can correspond to rectangular cells along $\underset{\sim}{k}_m^{(b)}$ and $\underset{\sim}{k}_m^{(t)}$, or two-dimensional rolls parallel to either $\underset{\sim}{k}_m^{(b)}$ or $\underset{\sim}{k}_m^{(t)}$. For $L_l \mid S_{mp}^{(b)} \mid > L_u \mid S_{mp}^{(t)} \mid$, two-dimensional rolls parallel to $\underset{\sim}{k}_m^{(b)}$ are preferred, while rolls parallel to $\underset{\sim}{k}_m^{(t)}$ are preferred for $L_l \mid S_{mp}^{(b)} \mid < L_u \mid S_{mp}^{(t)} \mid$. For $L_l \mid S_{mp}^{(b)} \mid = L_u \mid S_{mp}^{(t)} \mid$ and for the case where $\underset{\sim}{k}_m^{(b)}$ is inclined with respect to $\underset{\sim}{k}_m^{(t)}$, two-dimensional rolls along either $\underset{\sim}{k}_m^{(b)}$ or $\underset{\sim}{k}_m^{(t)}$ and rectangular pattern convection, whose wave

vectors are along $\underset{\sim}{k}_m^{(b)}$ and $\underset{\sim}{k}_m^{(t)}$, can be preferred since they all correspond to the same minimum R. The actual preferred solution can then due to initial conditions. This later rectangular pattern is converted to that for the preferred rolls along $\underset{\sim}{k}_m^{(b)}$ for $\underset{\sim}{k}_m^{(t)} = \underset{\sim}{k}_m^{(b)}$.

It should be noted that the magnitude of either $| S_{mp}^{(b)} |$ or $| S_{mp}^{(t)} |$ is the same for all possible values of the subscripts m and p under consideration. It turns out that this result also holds for the general case of arbitrary $N^{(b)}$ and $N^{(t)}$.

Example 2. $N^{(b)} = N^{(t)} = 1, \alpha^{(b)} = 2\alpha_c$ and $\alpha^{(t)} < 2\alpha_c$. The expression in the right hand side of (4.5) can be non-zero only if

$$\phi_{mp}^{(b)} = -1 \text{ or } \quad \phi_{mp}^{(t)} = \alpha^{(t)}/(2\alpha_c).$$

This result implies that the possible preferred solution can correspond to two-dimensional rolls, rectangular pattern and 6-sided polygonal pattern. For $L_l \mid S_{mp}^{(b)} \mid > L_u \mid S_{mp}^{(t)} \mid$, two-dimensional rolls along $\underset{\sim}{k}_m^{(b)}$ are preferred, while rectangular pattern convection, whose wave vectors are inclined at an angle $\omega_t/2$ to $\underset{\sim}{k}_m^{(t)}$, is preferred for $L_l \mid S_{mp}^{(b)} \mid > L_u \mid S_{mp}^{(t)} \mid$. The angle ω_t between two adjacent wave vectors of such rectangular pattern convection is given by (1.2).

For $\alpha^{(t)} = \sqrt{2}\,\alpha_c$, these rectangular cells become square cells. For $L_l \mid S_{mp}^{(b)} \mid = L_u \mid S_{mp}^{(t)} \mid$ and for the case where the angle between $\underset{\sim}{k}_m^{(b)}$ and $\underset{\sim}{k}_m^{(t)}$ is different from ω_t, 2-dimensional rolls along $\underset{\sim}{k}_m^{(b)}$, rectangular cells inclined at angle $\omega_t/2$ to $\underset{\sim}{k}_m^{(t)}$ and 6-sided polygonal cells along $\underset{\sim}{k}_m^{(b)}$ inclined at angle $\omega_t/2$ to $\underset{\sim}{k}_m^{(t)}$ are all possible patterns. The realizable preferred pattern is then one of these patterns, which is due to initial conditions, since these patterns lead to the same minimum value of R. However, for $L_l \mid S_{mp}^{(b)} \mid = L_u \mid S_{mp}^{(t)} \mid$ and for the case where the angle between $\underset{\sim}{k}_m^{(b)}$ and $\underset{\sim}{k}_m^{(t)}$ is equal to ω_t, then two-dimensional rolls along $\underset{\sim}{k}_m^{(b)}$ are the only possible preferred pattern.

Example 3. $N^{(b)} = N^{(t)} = 1, \alpha^{(b)} < 2\alpha_c$ and $\alpha^{(t)} < 2\alpha_c$.The expression in the right hand side of (4.5) can be non-zero only if

$$\phi_{mp}^{(b)} = \alpha^{(b)}/(2\alpha_c) \quad \text{or} \quad \phi_{mp}^{(t)} = \alpha^{(t)}/(2\alpha_c).$$

This result implies that the possible preferred solution can correspond to rectangular pattern convection and multi-modal ($N = 4$) pattern convection. For $L_l \mid S_{mp}^{(b)} \mid > L_u \mid S_{mp}^{(t)} \mid$, rectangular cells inclined at an angle $\omega_b/2$ to $\underset{\sim}{k}_m^{(b)}$ are preferred, while rectangular cells inclined at angle $\omega_t/2$ to $\underset{\sim}{k}_m^{(t)}$ are preferred for $L_l \mid S_{mp}^{(b)} \mid < L_u \mid S_{mp}^{(t)} \mid$. The angle ω_b between two adjacent wave vectors of the former rectangular cells is given by (1.1).

While that for the later rectangular cells is given by (1.2). For $L_l \mid S_{mp}^{(b)} \mid = L_u \mid S_{mp}^{(t)} \mid$ and for the case where $\underset{\sim}{k}_m^{(b)}$ is along $\underset{\sim}{k}_m^{(t)}$ and $\omega_t = \omega_b$, then rectangular cells inclined at angle $\omega_b/2$ to $\underset{\sim}{k}_m^{(b)}$ are preferred. For $L_l \mid S_{mp}^{(b)} \mid = L_u \mid S_{mp}^{(t)} \mid$ and for the case where $\underset{\sim}{k}_m^{(b)}$ is inclined at angle $(\omega_t - \omega_b)/2$ with respect to $\underset{\sim}{k}_m^{(t)}$, then 6-sided polygonal cells inclined at angles $\omega_b/2$ and $\omega_t/2$ with respect to $\underset{\sim}{k}_m^{(b)}$ and $\underset{\sim}{k}_m^{(t)}$, respectively, are preferred. For $L_l \mid S_{mp}^{(b)} \mid = L_u \mid S_{mp}^{(t)} \mid$ and for the case where $\underset{\sim}{k}_m^{(b)}$ is inclined to $\underset{\sim}{k}_m^{(t)}$ at angle different from $(\omega_t - \omega_b)/2$, then multi-modal ($N = 4$) cells inclined at angles $\omega_b/2$ and $\omega_t/2$ with respect to $\underset{\sim}{k}_m^{(b)}$ and $\underset{\sim}{k}_m^{(t)}$, respectively, are preferred.

Example 4. $N^{(b)} = 2, N^{(t)} = 1$ and $\alpha^{(b)} = \alpha^{(t)} = 2\alpha_c$. For $\mid L_u\sqrt{2}S_{mp}^{(t)} \mid > \mid L_l S_{mp}^{(b)} \mid$, two-dimensional rolls along $\underset{\sim}{k}_m^{(t)}$ are preferred. For $\mid L_l S_{mp}^{(b)} \mid > \mid L_u\sqrt{2}S_{mp}^{(t)} \mid$ and for the case where $\underset{\sim}{k}_m^{(t)}$ are inclined with respect to $\underset{\sim}{k}_m^{(b)}$, then rectangular pattern along $\underset{\sim}{k}_m^{(b)}$ is preferred, while two-dimensional rolls along $\underset{\sim}{k}_m^{(t)}$ are preferred if $\underset{\sim}{k}_m^{(t)}$ are along either $\underset{\sim}{k}_1^{(b)}$ (or $\underset{\sim}{k}_{-1}^{(b)}$) or $\underset{\sim}{k}_2^{(b)}$ (or $\underset{\sim}{k}_{-2}^{(b)}$). For $\mid L_l S_{mp}^{(b)} \mid = \mid L_u\sqrt{2}S_{mp}^{(t)} \mid$ and for the case where $\underset{\sim}{k}_m^{(t)}$ are inclined with respect to $\underset{\sim}{k}_m^{(b)}$, then 6-sided polygonal pattern along $\underset{\sim}{k}_m^{(b)}$ and $\underset{\sim}{k}_m^{(t)}$ is preferred, while two-dimensional rolls along $\underset{\sim}{k}_m^{(t)}$ are preferred if $\underset{\sim}{k}_m^{(t)}$ is along $\underset{\sim}{k}_m^{(b)}$.

Example 5. $N^{(b)} = 2, N^{(t)} = 1, \alpha^{(t)} = 2\alpha_c$, and $\alpha^{(b)} < 2\alpha_c$. Let us designate the angle between $\underset{\sim}{k}_1^{(b)}$ and $\underset{\sim}{k}_2^{(b)}$ by $\gamma_{12}^{(b)}$. For $\mid L_l S_{mp}^{(b)} \mid > \mid L_u\sqrt{2}S_{mp}^{(t)} \mid$ and for the case where $\gamma_{12}^{(b)} = 90°$ and $\alpha^{(b)} = \sqrt{2}\alpha_c$,

square pattern convection is preferred, while multi-modal ($N = 4$) pattern convection is preferred for $\gamma_{12}^{(b)} \neq 90°$ or for $\gamma_{12}^{(b)} = 90°$ and $\alpha^{(b)} \neq \sqrt{2}\,\alpha_c$. These results are valid, provided that $\underset{\sim}{k}_m^{(t)}$ is not along any wave vector of the resulting flow pattern, otherwise two-dimensional rolls along $\underset{\sim}{k}_m^{(t)}$ are preferred. Rolls along $\underset{\sim}{k}_m^{(t)}$ are also preferred for $| L_u\sqrt{2}S_{mp}^{(t)} | > L_l S_{mp}^{(b)} |$. For $| \sqrt{2}L_u S_{mp}^{(t)} | = | L_l S_{mp}^{(b)} |$, 6-sided polygonal (for $\gamma_{12}^{(b)} = 90°$ and $\alpha^{(b)} = \sqrt{2}\,\alpha_c$) and multi-modal ($N = 5$) (for $\alpha^{(b)} = \sqrt{2}\,\alpha_c$) patterns are preferred. This result is valid only if $\underset{\sim}{k}_m^{(t)}$ is not along any $\underset{\sim}{k}_m^{(b)}$, otherwise rectangular pattern along $\underset{\sim}{k}_m^{(t)}$ and inclined at angle $\cos^{-1}(\alpha^{(b)}/2\alpha_c)$ to $\underset{\sim}{k}_m^{(b)}$ is the preferred one.

The five examples presented above can be extended to arbitrary $N^{(b)}$ and $N^{(t)}$ and for the case where the boundary patterns are regular. We assume that $\alpha^{(b)} \leq 2\alpha_c$ and, $\alpha^{(t)} \leq 2\alpha_c$,. For

$$(L_l/L_u) > | (S_{mp}^{(t)}/S_{mp}^{(b)}) | (N^{(b)}/N^{(t)})^{1/2} \equiv S_{bt} \tag{4.10}$$

and for the case where none of $\underset{\sim}{k}_m^{(t)}$ are along any of $\underset{\sim}{k}_p^{(b)}$ for all possible m and p, then multi-modal convection pattern ($N = 2,... 2S$) are all possible for the case where $\gamma_{mp}^{(b)} = 90°$ for S number of times. Here $\gamma_{mp}^{(b)}$ denotes the angle between $\underset{\sim}{k}_m^{(b)}$ and $\underset{\sim}{k}_p^{(b)}$. For values of $\gamma_{mp}^{(b)}$ other than 90° for all m and p, then multi-modal convection patterns (with $N = 2,\ldots,2N^{(b)}$) are all possible preferred patterns for $\alpha^{(b)} < 2\alpha_c$, while multi-modal convection patterns with ($N = 1,\ldots,N^{(b)}$) are all possible preferred patterns for $\alpha^{(b)} = 2\alpha_c$. These later patterns are along subsets of $\underset{\sim}{k}_m^{(b)}$. If M number of $\underset{\sim}{k}_m^{(b)}$ are along M number of $\underset{\sim}{k}_p^{(t)}$, then the above results are applicable for the boundary modulations consisting of these M vectors, provided $N^{(b)}$ is replaced by M. If the inequality in (4.10) is reversed, then the above results are applicable, provided ($\underset{\sim}{k}_m^{(b)}, \underset{\sim}{k}_m^{(t)}$) and ($N^{(b)}, N^{(t)}$) are replaced, respectively ($\underset{\sim}{k}_m^{(t)}, \underset{\sim}{k}_m^{(b)}$) and ($N^{(t)}, N^{(b)}$). Consider now the case where the inequality in (4.10) is replaced by equality symbol. For $\alpha^{(b)} = \alpha^{(t)} = 2\alpha_c$ and for the case where none of $\underset{\sim}{k}_m^{(t)}$ are along any of $\underset{\sim}{k}_p^{(b)}$ for all possible m and p, then multi-modal ($N = 1,\ldots,N^{(b)} + N^{(t)}$) patterns along $\underset{\sim}{k}_m^{(b)}$ and $\underset{\sim}{k}_m^{(t)}$ are all possible preferred patterns since all lead to the same minimum R. The

preferred one is then due to initial condition. If M number of $\underset{\sim}{k}_m^{(t)}$ are along M number of $\underset{\sim}{k}_p^{(b)}$, then the above results are valid for these M vectors, provided that $N^{(b)}+N^{(t)}$ is replaced by M. For $\alpha^{(b)}=\alpha^{(t)}<2\alpha_c$, the above results are applicable for multi-modal ($N=2,\ldots,(2N^{(b)}+2N^{(t)})$) patterns, provided $\gamma_{mp}^{(b)}\neq 90°$ (for all m and p). If $\gamma_{mp}^{(b)}=90°$ for S number of times, then multi-modal ($N=2,\ldots,2S$) patterns are all possible. For $\alpha^{(b)}<2\alpha_c$, $\alpha^{(t)}=2\alpha_c$, $\gamma_{mp}^{(b)}\neq 90°$ (for all m and p) and for the case where none of $\underset{\sim}{k}_m^{(t)}$ are along any of $\underset{\sim}{k}_p^{(b)}$ for all possible m and p, then multi-modal ($N=1,\ldots,(2N^{(b)}+N^{(t)})$) patterns are all possible preferred patterns since all lead to the same minimum R. The initial condition can then select the preferred pattern from these patterns. If $\gamma_{mp}^{(b)}=90°$ for S number of times, then multi-modal ($N=2,\ldots,2S$) pattern are all possible. For $\alpha^{(b)}\neq\alpha^{(t)}<2\alpha_c$, $\alpha^{(b)}<2\alpha_c$, $\gamma_{mp}^{(b)}\neq 90°$, $\gamma_{mp}^{(t)}\neq 90°$ (for all m and p) and for the case where none of $\underset{\sim}{k}_m^{(t)}$ are along any of $\underset{\sim}{k}_p^{(b)}$ for all possible m and p, then multi-modal ($N=2,\ldots,(2N^{(b)}+2N^{(t)})$) patterns are all possible preferred patterns since all lead to the same minimum R, and the preferred one is due to initial condition. If $\gamma_{mp}^{(b)}=90°$ (or $\gamma_{mp}^{(t)}=90°$ or $\gamma_{mp}^{(bt)}=90°$) for S number of times, then multi-modal ($N=2,\ldots,2S$) patterns are all possible. In the above, $\gamma_{mp}^{(t)}$ denotes the angle between $\underset{\sim}{k}_m^{(t)}$ and $\underset{\sim}{k}_p^{(t)}$, while $\gamma_{mp}^{(bt)}$ denotes the angle between $\underset{\sim}{k}_m^{(b)}$ and $\underset{\sim}{k}_p^{(t)}$. Diagram 2 provides types of the flow patterns that are preferred under certain ranges of the modulation amplitudes and under certain orientations and magnitudes of the modulation wave vectors.

5. Discussion

As we pointed out in section two and was also shown in R93 for a porous layer with boundary modulation on the lower wall only, the present problem does not lead to different qualitative results from those for the problem where the lower and upper boundaries' locations are at $z=-1/2+\delta_l h_l(x,y)$ and $z=1/2+\delta_u h_u(x,y)$, respectively. Walton (1982) has shown similar results for the case of a horizontal fluid layer with slowly increasing depth. The boundaries corrugated problem can incorporate the effects of roughness elements of arbitrary

shapes h_l and h_u on the lower and upper boundaries, respectively, and the expressions (3.9a,b) for h_l and h_u are still valid, provided that $N^{(b)}$ and $N^{(t)}$ may tend to infinity and that $\alpha_m^{(b)}$ and $\alpha_m^{(t)}$ may not all have the same value. This extension of the problem can be easily analyzed by dividing the boundary modulations modes into two groups of the two different types considered in sections 3 and 4. Hence, the results presented in these two sections are applicable for each of these two groups of modes. Since the preferred flow pattern corresponds to the smallest value of R and (4.3) holds for the results presented in section 4, then the preferred flow pattern is due to the results presented in section 4 for $R_{01} < 0$, while the preferred flow pattern is due to the results presented in section 3 for $R_{01} > 0$.

Kelly and Pal (1976, 1978) and Pal and Kelly (1978) investigated onset of two-dimensional Rayleigh-Bénard convection with one-dimensional boundary modulations in the form of sine wave in one direction. They found that heat transported by convection can be enhanced, $R_{01} = 0$ for $\alpha_n^{(b)} \neq 2\alpha_c$, while $R_{01} < 0$ for $\alpha_n^{(b)} = 2\alpha_c$. Their case corresponds to two-dimensional flow with one-dimensional boundary modulation version of the present study with $l_l C_n^{(b)} > 0$ and $L_u C_n^{(t)} > 0$. As we discussed in sections 3 and 4, we found that heat transported by convection can be enhanced by boundary modulations in some ranges of L_l^* and L_u^*, $R_{01} \neq 0$ only for $\alpha_n^{(b)} \leq 2\alpha_c$ and that $R_{01} < 0$ for $L_l C_n^{(b)} > 0$ and $L_u C_n^{(t)} > 0$. Hence, our results cover those due to these authors.

Krettenauer and Schumann (1989) investigated by direct numerical simulations the problem of Rayleigh-Benard convection for the case where the lower boundary height varies sinusoidally in one direction only. For the subcritical flow case, they found that rolls along the wavy surface are the form of convection for $\alpha_n^{(b)} = \alpha_c$, while rectangular pattern evolved for the supercritical flow with one surface wave allowed in the computational box. Similar to these results were covered by the present results for $N^{(b)} = 1 (L_l > L_u)$ derived from example 1 given in section 3 and example 3 given in section 4. Krettenauer and Schumann (1992) extended their model to turbulent regime. They found, in particular, that the motion structure persists longer

over wavy terrain than over flat surface, three-dimensional motions are enforced by terrain and the boundary modulation is more effective for longer wavelength of the surface wave. These results are consistent with the present results.

Although there have been studies on the problem of convection in a horizontal layer with one-dimensional spatially periodic temperature (Kelly and Pal, 1978; Pal and Kelly, 1978; Krettenauer and Schumann, 1989; Yoo and Kim, 1991), these studies were either for two-dimensional flow case or for $N^{(b)} = N^{(t)} = 1$ only and thus could not investigate the problem of preferred flow pattern for $N^{(b)} \geq 1$ and $N^{(t)} \geq 1$ which is essentially a collection of infinite number of three-dimensional flow problems. It turns out from the present results that the mo st surprising results presented in section 3 correspond to the cases where $N^{(b)} > 1$ or $N^{(t)} > 1$, while the surprising results presented in section 4 correspond to the cases where $N^{(b)} \geq 1$ and $N^{(t)} \geq 1$ ·

6. Conclusion

The main results of the present study lead to the following conclusion which is described briefly here. I) For the case of resonant wavelength excitation and for arbitrary number of the modes representing the boundary modulations, multi-modal (N = J) pattern convection is preferred, where J is the number of modes representing the preferred flow pattern and is functions of the modulation amplitudes. Depending on the particular range of the modulation amplitudes, the wave vectors of the preferred flow pattern are along some of the modulation wave vectors. for $j \leq 3$, the preferred flow pattern is periodic, while for $j > 3$, it is generally quasi-periodic. II) For the case of non-resonant wavelength excitation and for arbitrary number of the modes representing the boundary modulations, several multi-modal (N = S) flow patterns correspond to the minimum value of R, where S is the number of modes representing the flow pattern and takes several different values one corresponding to each of these flow patterns. Also, S is functions of modulation amplitudes and of magnitudes and orientations of modulation wave vectors. For particular range of modulation amplitudes and for the case where the magnitudes of

Flow patterns

the modulation wave vectors are equal to $2\alpha_c$, are along the modulation wave vectors. For other range of modulation amplitudes and for cases where the magnitudes of the modulation wave vectors are not equal to $2\alpha_c$, the resulting multi-modal flow patterns are inclined to the modulation wave vectors. The angles between the wave vectors of the resulting flow patterns and the modulation wave vectors are generally functions of the magnitudes and orientations of the modulation wave vectors.

Appendix

The order $\varepsilon^0\delta^1$ system is of the form

$$\left.\begin{aligned} &\Delta_2(\nabla^4\phi_{01}-\theta_{01})=0, \quad \nabla^2\theta_{01}-R_c\Delta_2\phi_{01}=0,\\ &\phi_{01}=\frac{\partial\phi_{01}}{\partial z}=\theta_{01}-R_c h_l=0 \quad \text{at } z=-\frac{1}{2},\\ &\phi_{01}=\frac{\partial\phi_{01}}{\partial z}=\theta_{01}-R_c h_u=0 \quad \text{at } z=-\frac{1}{2}, \end{aligned}\right\} \tag{A.1}$$

The functions F_{ln}, G_{ln}, F_{un} and G_{un} are the solutions of the following system:

$$\left.\begin{aligned} &\left[D^2-(\alpha_n^{(b)})^2\right]^2 F_{ln}-G_{ln}=\left[D^2-(\alpha_n^{(t)})^2\right]^2 F_{un}-G_{un}=0,\\ &\left[D^2-(\alpha_n^{(b)})^2\right]G_{ln}+R_c(\alpha_n^{(b)})^2 F_{ln}=0\\ &\left[D^2-(\alpha_n^{(t)})^2\right]G_{un}+R_c(\alpha_n^{(t)})^2 F_{un}=0\\ &F_{ln}=DF_{ln}=G_{ln}-R_c=F_{un}=DF_{un}=G_{un}=0 \text{ at } z=-\frac{1}{2},\\ &F_{ln}=DF_{ln}=G_{ln}=F_{un}=DF_{un}=G_{un}-R_c=0 \text{ at } z=-\frac{1}{2}, \end{aligned}\right\} \tag{A.2}$$

where $D \equiv d/dz$. The solution to (A.2) is given below

$$[F_{ln}(z), G_{ln}(z)] = \sum_{i=1}^{6} d_i \left\{ 1, \left[r_i^2-(\alpha_n^{(b)})^2\right]^2 \right\} \exp(r_i z), \tag{A.3}$$

where

$$r_1=-r_4=\left\{(\alpha_n^{(b)})^2-\left[R_c(\alpha_n^{(b)})^2\right]^{1/3}\right\}^{1/2},$$

$$r_2=-r_5=\left\{(\alpha_n^{(b)})^2+\left[R_c(\alpha_n^{(b)})^2\right]^{1/3}\exp\left(-\frac{1}{3}i\pi\right)\right\}^{1/2},$$

$$r_3=-r_6=\left\{(\alpha_n^{(b)})^2+\left[R_c(\alpha_n^{(b)})^2\right]^{1/3}\exp\left(\frac{1}{3}i\pi\right)\right\}^{1/2},$$

and the coefficients $d_i (i = 1, \ldots, 6)$ satisfy the following algebraic system for constants $\gamma_1 = 0$ and $\gamma_2 = 1$:

$$\sum_{i=1}^{6} d_i \exp(r_i/2) = \sum_{i=1}^{6} d_i \exp(-r_i/2) = 0,$$

$$\sum_{i=1}^{6} d_i r_i \exp(r_i/2) = \sum_{i=1}^{6} d_i r_i \exp(-r_i/2) = 0,$$

$$\sum_{i=1}^{6} d_i \left[r_i^2 - (\alpha_n^{(b)})^2 \right]^2 \exp\left(\frac{r_i}{2} \right) - \gamma_1 R_c = 0,$$

$$\sum_{i=1}^{6} d_i \left[r_i^2 - (\alpha_n^{(b)})^2 \right]^2 \exp\left(-\frac{r_i}{2} \right) - \gamma_2 R_c = 0.$$

The functions $F_{un}(z)$ and $G_{un}(z)$ have the same form as $F_{\ln}(z)$ and $G_{\ln}(z)$, respectively, provided d_i, r_i and $\alpha_n^{(b)}$ are replaced by $\tilde{d}_i, \tilde{r}_i$ and $\alpha_n^{(t)}$, respectively. The expressions for $\tilde{r}_i$ and $\tilde{d}_i$ are the same as those for r_i and d_i, respectively, provided $\alpha_n^{(b)}, \gamma_1$ and γ_2 are replaced respectively by $\alpha_n^{(t)}$, 1 and 0.

The expression for $S_{mp}^{(b)}$ introduced in (4.5) is given below:

$$S_{mp}^{(b)} = \{ < gfG'_{lp} > \alpha_c^2 - < gf'G_{lp} > \alpha_c \alpha_p^{(b)} \phi_{mp}^{(b)} + < gg'F_{lp} > .$$

$$\cdot \alpha_p^{(b)} (\alpha_p^{(b)} + 2\alpha_c \phi_{mp}^{(b)}) + (R_c/p) [< f(f'F''_{lp} + f''F'_{lp}) > .$$

$$\cdot \alpha_c \alpha_p^{(b)} \phi_{mp}^{(b)} \left(\alpha_c^2 + (\alpha_p^{(b)})^2 + 2\alpha_c \alpha_p^{(b)} \phi_{mp}^{(b)} \right) - < f(f'F''_{lp} + fF'''_{lp}) > .$$

$$\cdot \alpha_c^2 \left((\alpha_p^{(b)})^2 + \alpha_c \alpha_p^{(b)} \phi_{mp}^{(b)} \right) + < ff'F_{lp} > \alpha_c (\alpha_p^{(b)})^2 .$$

$$\cdot (\alpha_c + \alpha_p^{(b)} \phi_{mp}^{(b)}) \left(\alpha_c^2 + (\alpha_p^{(b)})^2 + 2\alpha_c \alpha_p^{(b)} \phi_{mp}^{(b)} \right)$$

$$- < f^2 F'_{lp} > \alpha_c^2 \alpha_p^{(b)} (\alpha_p^{(b)} + \alpha_c \phi_{mp}^{(b)}) (\alpha_c^2 + (\alpha_p^{(b)})^2 +$$

$$2\alpha_c \alpha_p^{(b)} \phi_{mp}^{(b)}) - < f(F_{lp} f''' + F'_{lp} f'') > (\alpha_p^{(b)})^2 . \cdot \alpha_c (\alpha_c + \alpha_p^{(b)} \phi_{mp}^{(b)})] \} / F_0, \qquad (A.4)$$

where prime denotes differentiation with respect to z. The expression for $S_{mp}^{(t)}$ introduced in (4.5) has the same form as (A.4) for $S_{mp}^{(b)}$, provided $\alpha_p^{(b)}, \phi_{mp}^{(b)}, F_{lp}$ and G_{lp} are replaced, respectively, $\alpha_p^{(t)}, \phi_{mp}^{(t)}, F_{up}$ and G_{up}.

References

Busse, F. H. 1978 Nonlinear properties of thermal convection. Rep. on Prog. in Phys. **41**, 1929-1967.

Chandrasekhar, S. 1961 Hydynamic and hydromagnetic stability. Oxford Univ. Press.

Kelly, R. E. and Pal, D. 1976 Thermal convection induced between non-uniformity heated horizontal surfaces. Proc. 1976 Heat Transfer and Fluid Mech. Inst., pp. 1-17. Stanford Univ. Press.

Kelly, R. E. and Pal, D. 1978 Thermal convection with spatially periodic boundary conditions: resonant wavelength excitation. *J. Fluid Mech.* **86**, 433-456.

Krettenauer, K. and Schumann, U. 1989 Direct numerical simulation of thermal convection over a wavy surface. *Met. Atmos. Phys.* **41**, 165-179.

Krettenauer, K. and Schumann, U. 1992 Numerical simulation of turbulent convection over wavy terrain. *J. Fluid Mech.* **237**, 261-299.

Malkus, W.V.R. and Veronis, G. 1958 Finite amplitude cellular convection. *J. Fluid Mech.* **4**, 225-260.

Pal, D. and Kelly, R. E. 1978 Thermal convection with spatially periodic nonuniform heating: nonresonant wavelength excitation. Proc. 6th Int. Heat Transfer Conf. Toronto, 235-238.

Pismen, L. M. 1087 Bifurcation of quasiperiodic and nonstationary pattern under external forcing. *Phys. Rev. Lett.* **59**, 2740-2743.

Riahi, N. 1985 Nonlinear thermal convection with finite conducting boundaries. *J. Fluid Mech.* **152**, 113-123.

Riahi, D. N. 1993 Preferred pattern of convection in a porous layer with a spatially non-uniform boundary temperature. *J. Fluid Mech.* **246**, 529-543.

Schlüter, A., Lortz, D. and Busse, F. H. 1965 On the stability of finite amplitude convection. *J. Fluid Mech.* **23**, 129-144.

Tavantzis, J., Reiss, E. L. and Matkowsky, B. J. 1978 On the smooth transition to convection. *SIAM J. Appl. Math.* **34**, 322-337.

Walton, I. C. 1982 On the onset of Rayleigh-Benard convection in a fluid layer of slowly increasing depth. *Stud. in Appl. Math.* **67**, 199-216.

Walton, I. C. 1983 The onset of cellular convection in a shallow two-dimensional container of fluid heated non-uniformly from below. *J. Fluid Mech.* **131**, 455-470.

Yoo, J. S. and Kim, M. U. 1991 Two-dimensional convection in a horizontal fluid layer with spatially periodic boundary temperatures. *Fluid Dyn. Res.* **7**, 181-200.

Diagram Captions

Diagram 1. Case of resonant wavelength excitation. It provides types of the flow patterns that are preferred under certain ranges of the modulation amplitudes and under certain orientations of the modulation wave vectors.

Diagram 2. Case of non-resonant wavelength excitation. It provides types of the flow patterns that are preferred as functions of the modulation amplitudes and of the orientations and magnitudes of the modulation wave vectors.

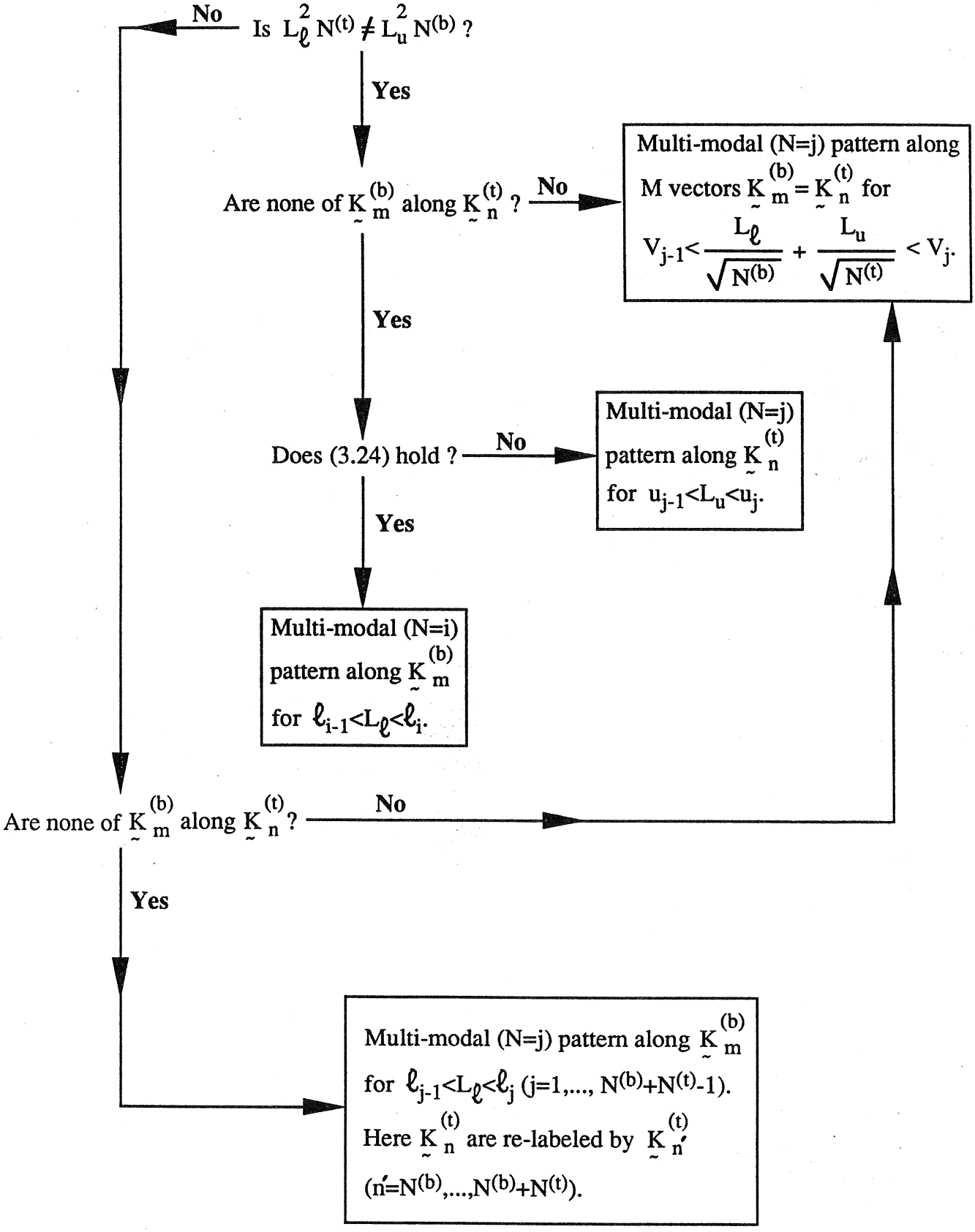
No
Is $L_\ell^2 N^{(t)} \neq L_u^2 N^{(b)}$?
Yes
Are none of $\underset{\sim}{K}_m^{(b)}$ along $\underset{\sim}{K}_n^{(t)}$?
No
Multi-modal (N=j) pattern along M vectors $\underset{\sim}{K}_m^{(b)} = \underset{\sim}{K}_n^{(t)}$ for $V_{j-1} < \frac{L_\ell}{\sqrt{N^{(b)}}} + \frac{L_u}{\sqrt{N^{(t)}}} < V_j$.
Yes
Does (3.24) hold ?
No
Multi-modal (N=j) pattern along $\underset{\sim}{K}_n^{(t)}$ for $u_{j-1} < L_u < u_j$.
Yes
Multi-modal (N=i) pattern along $\underset{\sim}{K}_m^{(b)}$ for $\ell_{i-1} < L_\ell < \ell_i$.
Are none of $\underset{\sim}{K}_m^{(b)}$ along $\underset{\sim}{K}_n^{(t)}$?
No
Yes
Multi-modal (N=j) pattern along $\underset{\sim}{K}_m^{(b)}$ for $\ell_{j-1} < L_\ell < \ell_j$ (j=1,..., $N^{(b)}+N^{(t)}-1$). Here $\underset{\sim}{K}_n^{(t)}$ are re-labeled by $\underset{\sim}{K}_{n'}^{(t)}$ ($n'=N^{(b)},...,N^{(b)}+N^{(t)}$).

Diag. 1

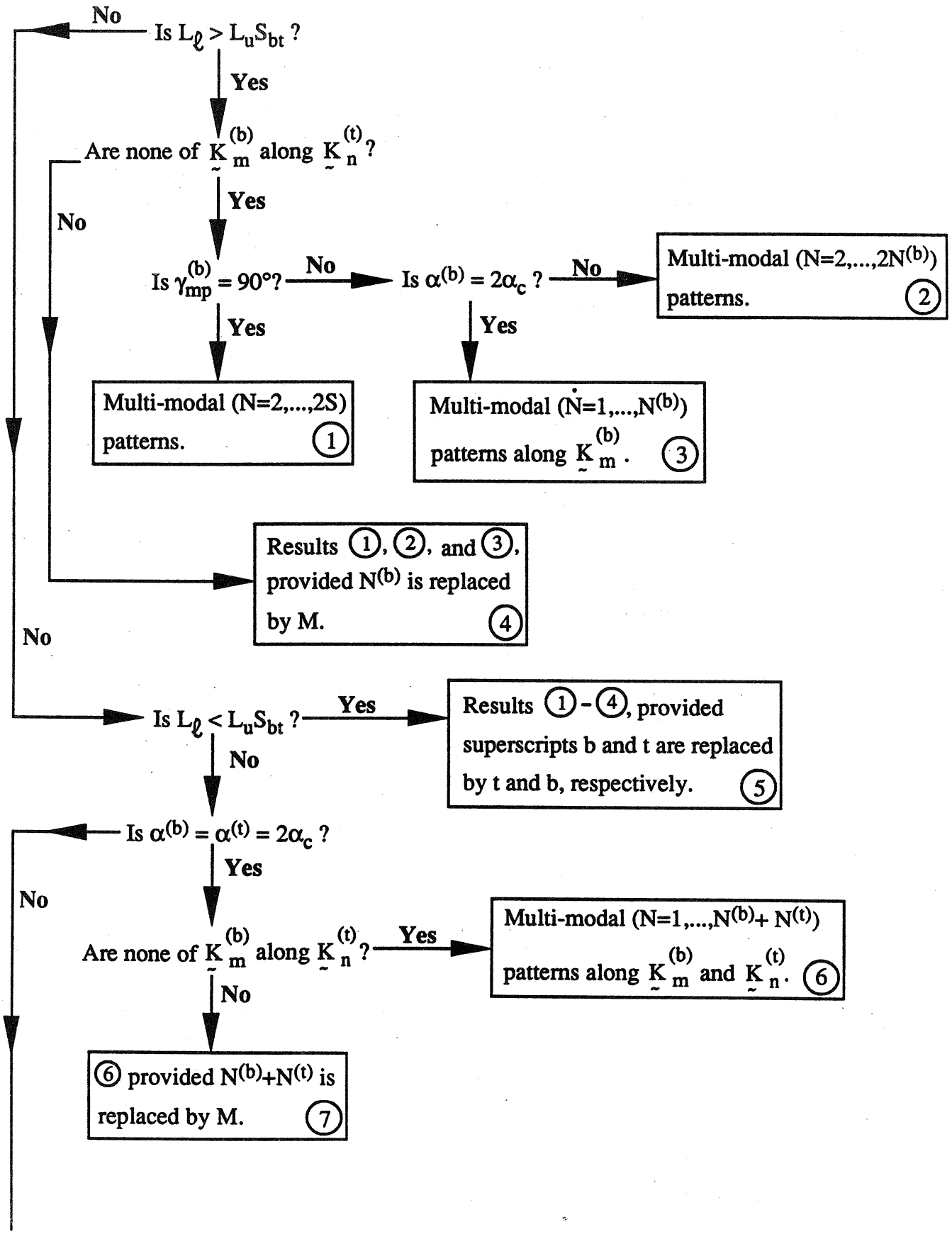
Is $L_\ell > L_u S_{bt}$?
No
Yes
Are none of $\underset{\sim}{K}_m^{(b)}$ along $\underset{\sim}{K}_n^{(t)}$?
Yes
No
Is $\gamma_{mp}^{(b)} = 90°$?
No
Is $\alpha^{(b)} = 2\alpha_c$?
No
Multi-modal (N=2,...,$2N^{(b)}$) patterns. (2)
Yes
Yes
Multi-modal (N=2,...,2S) patterns. (1)
Multi-modal (N=1,...,$N^{(b)}$) patterns along $\underset{\sim}{K}_m^{(b)}$. (3)
Results (1), (2), and (3), provided $N^{(b)}$ is replaced by M. (4)
No
Is $L_\ell < L_u S_{bt}$?
Yes
Results (1) - (4), provided superscripts b and t are replaced by t and b, respectively. (5)
No
Is $\alpha^{(b)} = \alpha^{(t)} = 2\alpha_c$?
Yes
No
Are none of $\underset{\sim}{K}_m^{(b)}$ along $\underset{\sim}{K}_n^{(t)}$?
Yes
Multi-modal (N=1,...,$N^{(b)}+ N^{(t)}$) patterns along $\underset{\sim}{K}_m^{(b)}$ and $\underset{\sim}{K}_n^{(t)}$. (6)
No
(6) provided $N^{(b)}+N^{(t)}$ is replaced by M. (7)

diag. 2

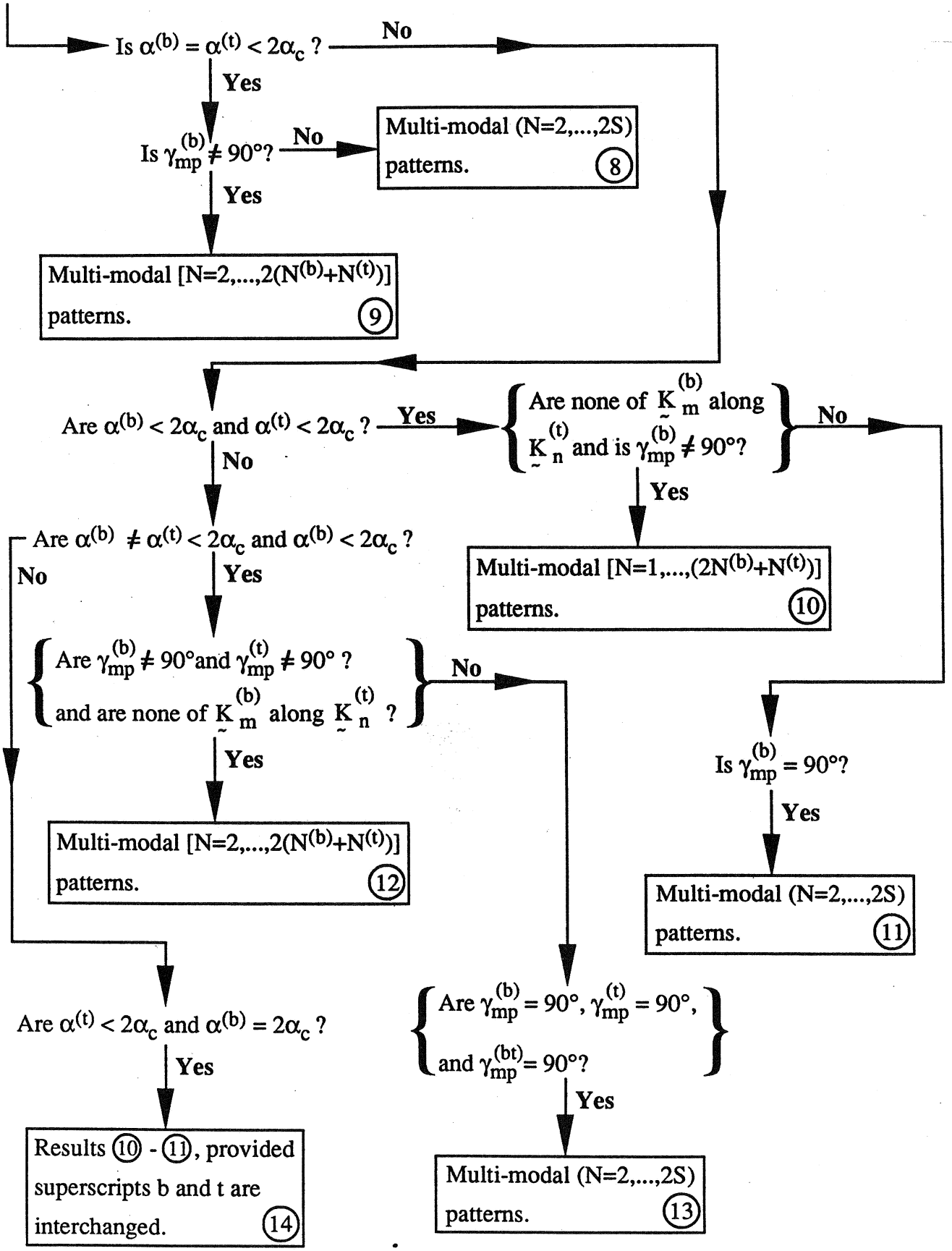
Is $\alpha^{(b)} = \alpha^{(t)} < 2\alpha_c$?
No
Yes
Is $\gamma_{mp}^{(b)} \neq 90°$?
No
Multi-modal (N=2,...,2S) patterns. (8)
Yes
Multi-modal [N=2,...,2($N^{(b)}$+$N^{(t)}$)] patterns. (9)
Are $\alpha^{(b)} < 2\alpha_c$ and $\alpha^{(t)} < 2\alpha_c$?
Yes
Are none of $\underset{\sim}{K}_m^{(b)}$ along $\underset{\sim}{K}_n^{(t)}$ and is $\gamma_{mp}^{(b)} \neq 90°$?
No
Yes
Multi-modal [N=1,...,(2$N^{(b)}$+$N^{(t)}$)] patterns. (10)
No
Are $\alpha^{(b)} \neq \alpha^{(t)} < 2\alpha_c$ and $\alpha^{(b)} < 2\alpha_c$?
Yes
Are $\gamma_{mp}^{(b)} \neq 90°$ and $\gamma_{mp}^{(t)} \neq 90°$?
and are none of $\underset{\sim}{K}_m^{(b)}$ along $\underset{\sim}{K}_n^{(t)}$?
No
Yes
Multi-modal [N=2,...,2($N^{(b)}$+$N^{(t)}$)] patterns. (12)
Is $\gamma_{mp}^{(b)} = 90°$?
Yes
Multi-modal (N=2,...,2S) patterns. (11)
Are $\alpha^{(t)} < 2\alpha_c$ and $\alpha^{(b)} = 2\alpha_c$?
Yes
Results (10) - (11), provided superscripts b and t are interchanged. (14)
Are $\gamma_{mp}^{(b)} = 90°$, $\gamma_{mp}^{(t)} = 90°$, and $\gamma_{mp}^{(bt)} = 90°$?
Yes
Multi-modal (N=2,...,2S) patterns. (13)

Cont. diag. 2

List of Recent TAM Reports

No.	Authors	Title	Date
707	Hsia, K. J., and J. Q. Huang	Curvature effects on compressive failure strength of long fiber composite laminates	Jan. 1993
708	Jog, C. S., R. B. Haber, and M. P. Bendsøe	Topology design with optimized, self-adaptive materials	Mar. 1993
709	Barkey, M. E., D. F. Socie, and K. J. Hsia	A yield surface approach to the estimation of notch strains for proportional and nonproportional cyclic loading	Apr. 1993
710	Feldsien, T. M., A. D. Friend, G. S. Gehner, T. D. McCoy, K. V. Remmert, D. L. Riedl, P. L. Scheiberle, and J. W. Wu	Thirtieth student symposium on engineering mechanics, J. W. Phillips, coord.	Apr. 1993
711	Weaver, R. L.	Anderson localization in the time domain: Numerical studies of waves in two-dimensional disordered media	Apr. 1993
712	Cherukuri, H. P., and T. G. Shawki	An energy-based localization theory: Part I—Basic framework	Apr. 1993
713	Manring, N. D., and R. E. Johnson	Modeling a variable-displacement pump	June 1993
714	Birnbaum, H. K., and P. Sofronis	Hydrogen-enhanced localized plasticity—A mechanism for hydrogen-related fracture	July 1993
715	Balachandar, S., and M. R. Malik	Inviscid instability of streamwise corner flow	July 1993
716	Sofronis, P.	Linearized hydrogen elasticity	July 1993
717	Nitzsche, V. R., and K. J. Hsia	Modelling of dislocation mobility controlled brittle-to-ductile transition	July 1993
718	Hsia, K. J., and A. S. Argon	Experimental study of the mechanisms of brittle-to-ductile transition of cleavage fracture in silicon single crystals	July 1993
719	Cherukuri, H. P., and T. G. Shawki	An energy-based localization theory: Part II—Effects of the diffusion, inertia and dissipation numbers	Aug. 1993
720	Aref, H., and S. W. Jones	Chaotic motion of a solid through ideal fluid	Aug. 1993
721	Stewart, D. S.	Lectures on detonation physics: Introduction to the theory of detonation shock dynamics	Aug. 1993
722	Lawrence, C. J., and R. Mei	Long-time behavior of the drag on a body in impulsive motion	Sept. 1993
723	Mei, R., J. F. Klausner, and C. J. Lawrence	A note on the history force on a spherical bubble at finite Reynolds number	Sept. 1993
724	Qi, Q., R. E. Johnson, and J. G. Harris	A re-examination of the boundary layer attenuation and acoustic streaming accompanying plane wave propagation in a circular tube	Sept. 1993
725	Turner, J. A., and R. L. Weaver	Radiative transfer of ultrasound	Sept. 1993
726	Yogeswaren, E. K., and J. G. Harris	A model of a confocal ultrasonic inspection system for interfaces	Sept. 1993
727	Yao, J., and D. S. Stewart	On the normal detonation shock velocity–curvature relationship for materials with large activation energy	Sept. 1993
728	Qi, Q.	Attenuated leaky Rayleigh waves	Oct. 1993
729	Sofronis, P., and H. K. Birnbaum	Mechanics of hydrogen–dislocation–impurity interactions: Part I—Increasing shear modulus	Oct. 1993
730	Hsia, K. J., Z. Suo, and W. Yang	Cleavage due to dislocation confinement in layered materials	Oct. 1993
731	Acharya, A., and T. G. Shawki	A second-deformation-gradient theory of plasticity	Oct. 1993
732	Michaleris, P., D. A. Tortorelli, and C. A. Vidal	Tangent operators and design sensitivity formulations for transient nonlinear coupled problems with applications to elasto-plasticity	Nov. 1993

(continued on next page)

List of Recent TAM Reports (cont'd)

No.	Authors	Title	Date
733	Michaleris, P., D. A. Tortorelli, and C. A. Vidal	Analysis and optimization of weakly coupled thermo-elasto-plastic systems with applications to weldment design	Nov. 1993
734	Ford, D. K., and D. S. Stewart	Probabilistic modeling of propellant beds exposed to strong stimulus	Nov. 1993
735	Mei, R., R. J. Adrian, and T. J. Hanratty	Particle dispersion in isotropic turbulence under the influence of non-Stokesian drag and gravitational settling	Nov. 1993
736	Dey, N., D. F. Socie, and K. J. Hsia	Static and cyclic fatigue failure at high temperature in ceramics containing grain boundary viscous phase: Part I—Experiments	Nov. 1993
737	Dey, N., D. F. Socie, and K. J. Hsia	Static and cyclic fatigue failure at high temperature in ceramics containing grain boundary viscous phase: Part II—Modelling	Nov. 1993
738	Turner, J. A., and R. L. Weaver	Radiative transfer and multiple scattering of diffuse ultrasound in polycrystalline media	Nov. 1993
739	Qi, Q., and R. E. Johnson	Resin flows through a porous fiber collection in pultrusion processing	Dec. 1993
740	Weaver, R. L., W. Sachse, and K. Y. Kim	Transient elastic waves in a transversely isotropic plate	Dec. 1993
741	Zhang, Y., and R. L. Weaver	Scattering from a thin random fluid layer	Dec. 1993
742	Weaver, R. L., and W. Sachse	Diffusion of ultrasound in a glass bead slurry	Dec. 1993
743	Sundermeyer, J. N., and R. L. Weaver	On crack identification and characterization in a beam by nonlinear vibration analysis	Dec. 1993
744	Li, L., and N. R. Sottos	Predictions of static displacements in 1–3 piezocomposites	Dec. 1993
745	Jones, S. W.	Chaotic advection and dispersion	Jan. 1994
746	Stewart, D. S., and J. Yao	Critical detonation shock curvature and failure dynamics: Developments in the theory of detonation shock dynamics	Feb. 1994
747	Mei, R., and R. J. Adrian	Effect of Reynolds-number-dependent turbulence structure on the dispersion of fluid and particles	Feb. 1994
748	Liu, Z.-C., R. J. Adrian, and T. J. Hanratty	Reynolds-number similarity of orthogonal decomposition of the outer layer of turbulent wall flow	Feb. 1994
749	Barnhart, D. H., R. J. Adrian, and G. C. Papen	Phase-conjugate holographic system for high-resolution particle image velocimetry	Feb. 1994
750	Qi, Q., W. D. O'Brien Jr., and J. G. Harris	The propagation of ultrasonic waves through a bubbly liquid into tissue: A linear analysis	Mar. 1994
751	Mittal, R., and S. Balachandar	Direct numerical simulation of flow past elliptic cylinders	May 1994
752	Anderson, D. N., J. R. Dahlen, M. J. Danyluk, A. M. Dreyer, K. M. Durkin, J. J. Kriegsmann, J. T. McGonigle, and V. Tyagi	Thirty-first student symposium on engineering mechanics, J. W. Phillips, coord.	May 1994
753	Thoroddsen, S. T.	The failure of the Kolmogorov refined similarity hypothesis in fluid turbulence	May 1994
754	Turner, J. A., and R. L. Weaver	Time dependence of multiply scattered diffuse ultrasound in polycrystalline media	June 1994
755	Riahi, D. N.	Finite-amplitude thermal convection with spatially modulated boundary temperatures	June 1994
756	Riahi, D. N.	Renormalization group analysis for stratified turbulence	June 1994
757	Riahi, D. N.	Wave-packet convection in a porous layer with boundary imperfections	June 1994